Evaluation on formability of complex concentrated alloys with different deformation mechanism

Current Status of Structural Materials
2020.04.13

Jeong-Won Yeh

Department of Materials Science and Engineering,
Seoul National University, Republic of Korea

Contents

Complex concentrated alloy: a new paradigm of alloy design

Conventional alloys | **Complex concentrated alloys**

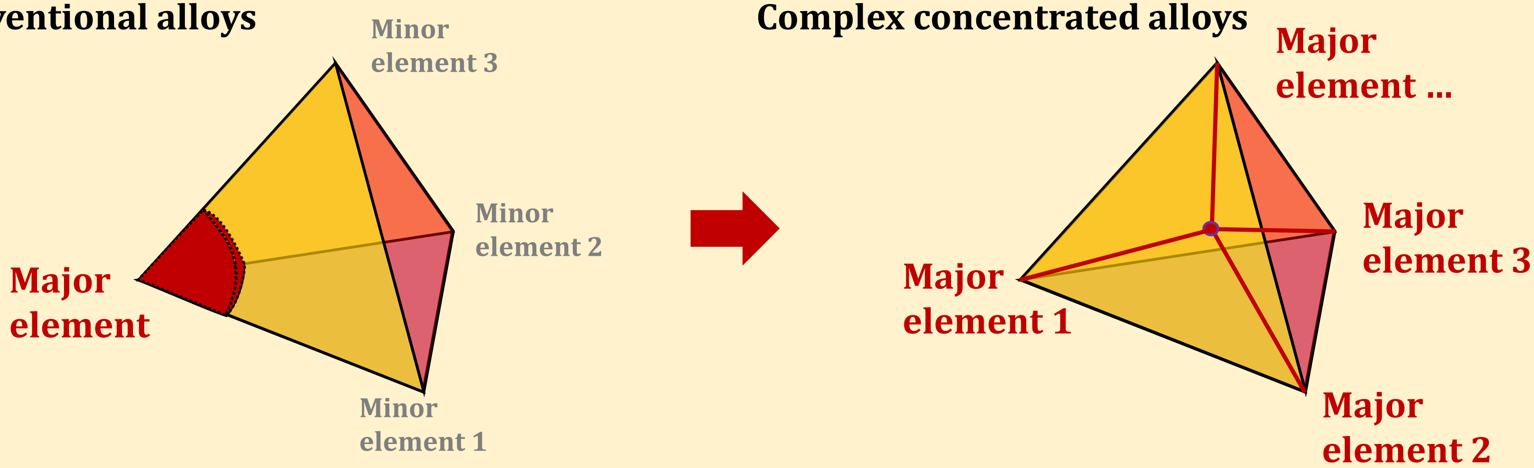

Ex) Fe, Cu, Al, Ti, Mg, Zr

Ex) $Al_{20}Co_{20}Cr_{20}Fe_{20}Ni_{20}$

number of elements ↑ ↔ ***configurational entropy*** ↑ →

$$\Delta S_{config.} = Rln(n)$$

- **Composition based definition (High entropy alloy)**

  Composed of **five or more principal elements** with the concentration of each element being between **5 - 35 at.%**.

- **Additional definition**

  Single-phase solid solution (or multiphase when consisting phases satisfy composition based or entropy based definitions.)

  (1) Thermodynamics : high entropy effect

  (2) Kinetics : sluggish diffusion effect

  (3) Structure : severe lattice distortion effect

  (4) Property : cocktail effect

L.J. Santodonato et al., Nature communications 6, 5964 (2015)

Representative complex concentrated alloy: cantor alloy

Cantor alloy: $Cr_{20}Mn_{20}Fe_{20}Co_{20}Ni_{20}$

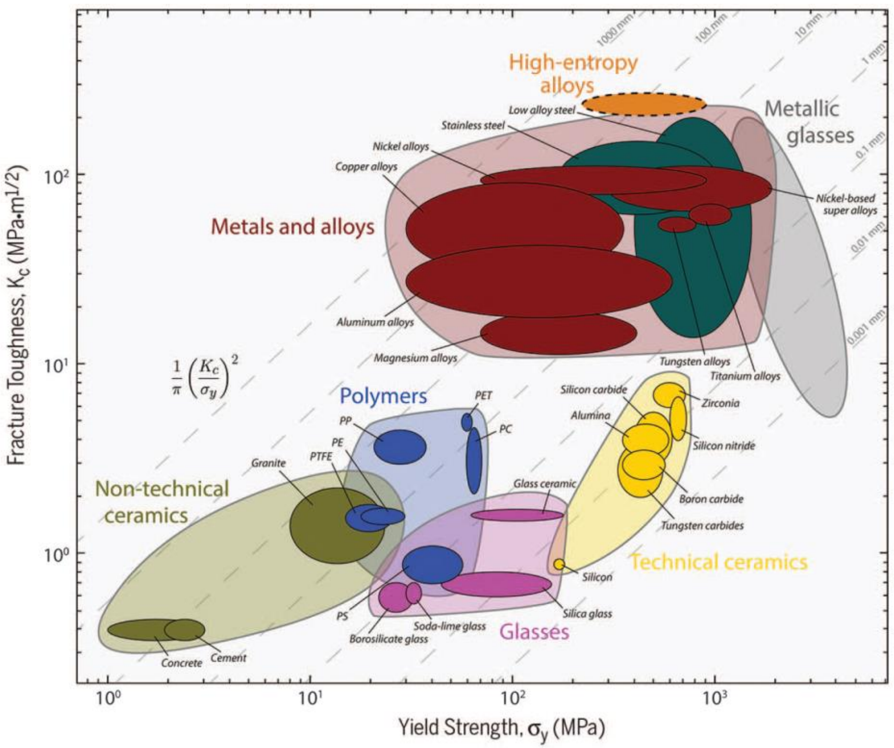

B.Gludovatz et al., Science 345, 1153 (2014)

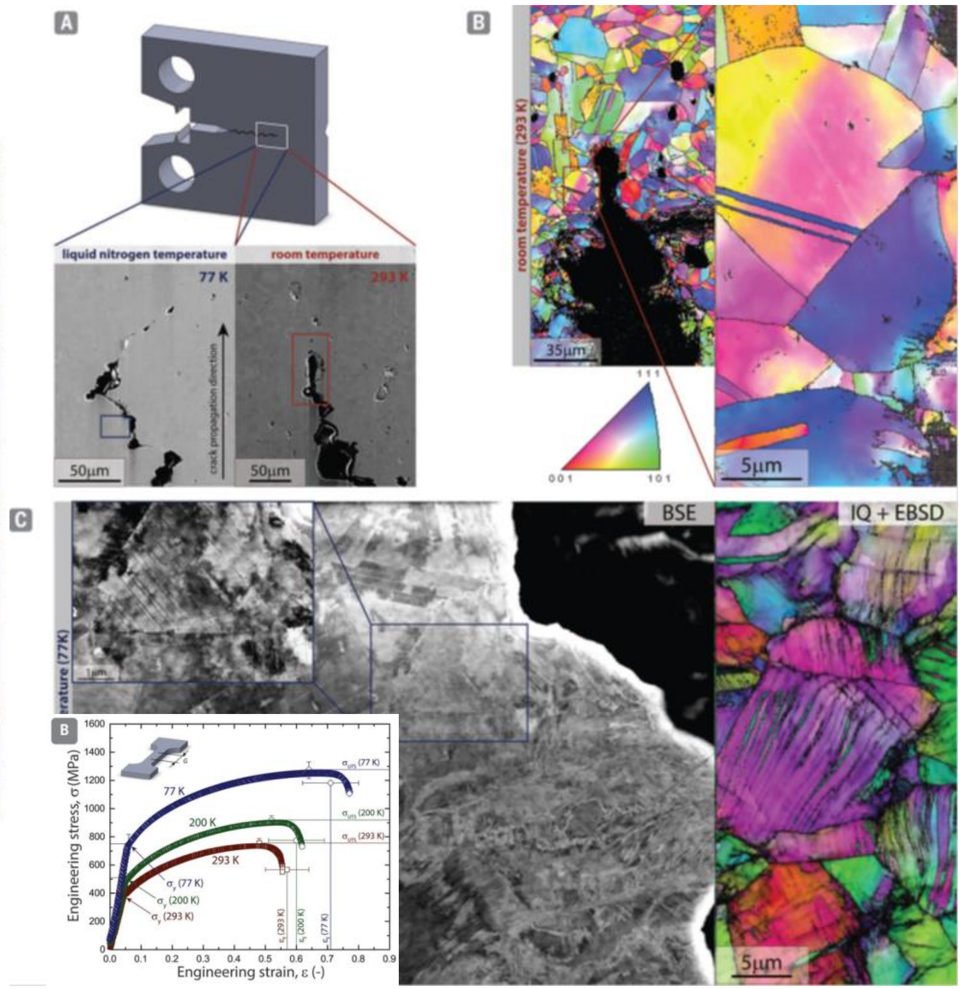

CCAs are expected to be structural materials

Formability evaluation is essential for using HEAs as structural materials.

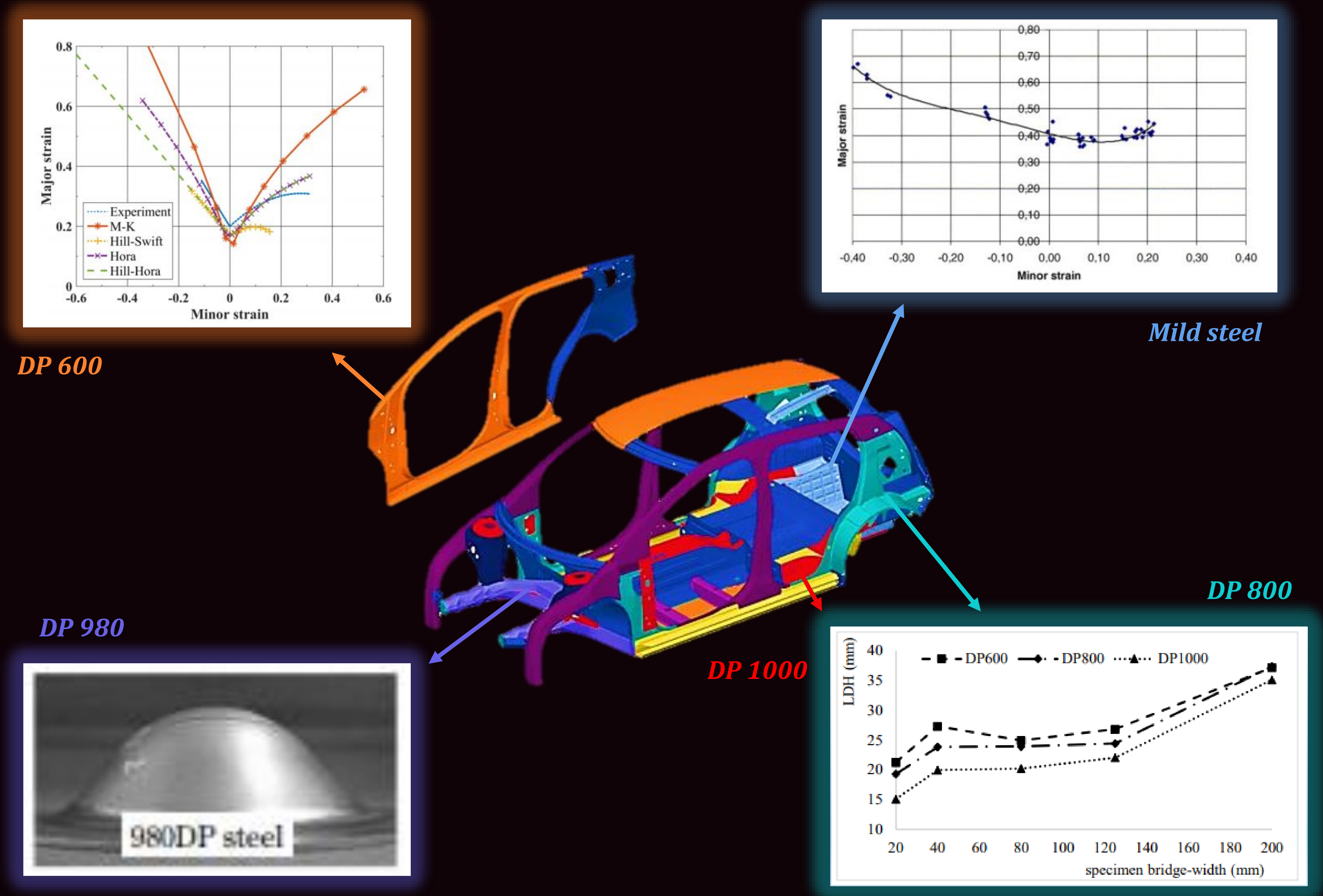

Necessity of formability test: Evaluation of formability

Evaluate formability

From uniaxial tensile test

- Yield stress ↓
- Ultimate tensile stress ↑
- Uniform elongation ↑
- Strain hardening ↑

$\hookrightarrow$ **$\sigma = K\sigma^n$, $d\sigma/d\varepsilon = nK\varepsilon^{n-1} = \sigma$**

or

$\varepsilon = n$

onset of necking occur at
strain = strain hardening exponent

Additional property

- Plastic instability
- Localized necking
- R-value
- Strain rate sensitivity

…

Formability tendency effected by additional property_TWIP940

K. Chung et al./ *International Journal of Plasticity 27(2011)52-81*

	Failure without stain localization		Failure with stain localization	
Material	TWIP940	AZ31B	AA5083-O	DP600
Thickness	1.47 mm	2.00 mm	1.60 mm	1.50 mm
m value	-0.007	0.008	-0.004	0.009
R_0 value	0.816	2.717	0.524	1.002
Calculated θ	56.16°	49.47°	59.61°	54.72°
Top view	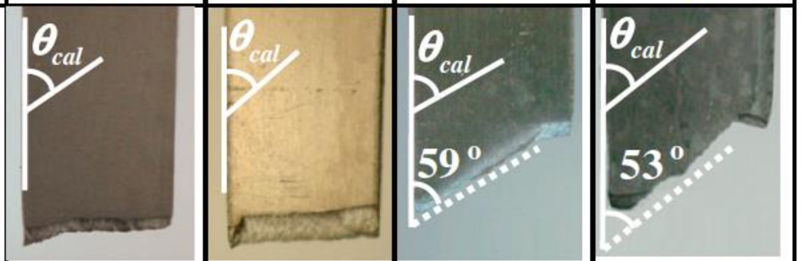			
Side view				

Fail without strain localization

+

Negative strain rate sensitivity

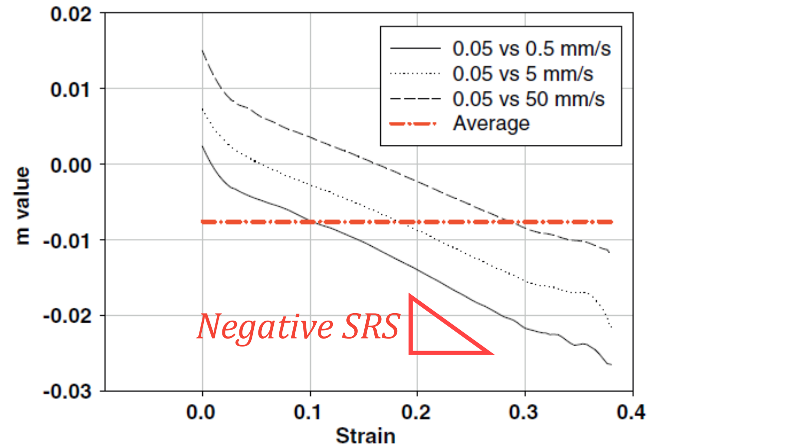

Variation of the m value of the TWIP940 steel with respect to strain and strain rate.

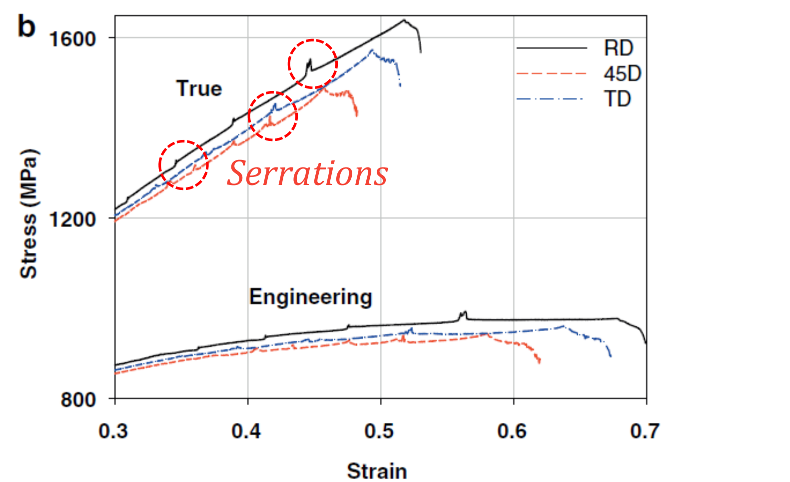

Magnified dynamic strain aging section of tensile curve of TWIP940

Fail without strain localization, – strain rate sensitivity(m): formability↓

CCAs Design with various deformation mechanism by SFE control

Dislocation

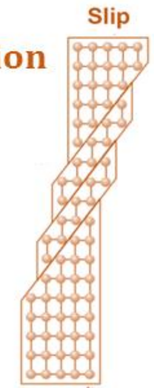

TWIP

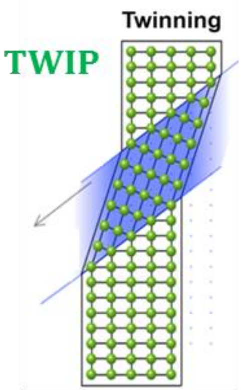

TRIP

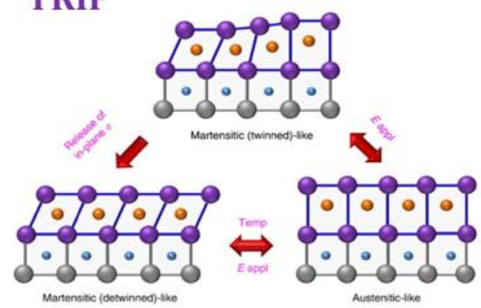

Dual phase

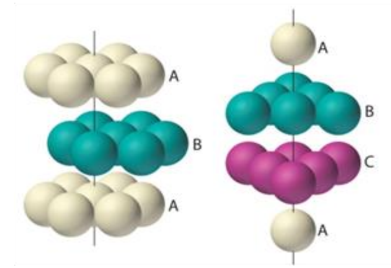

Decrease of Stacking Fault Energy

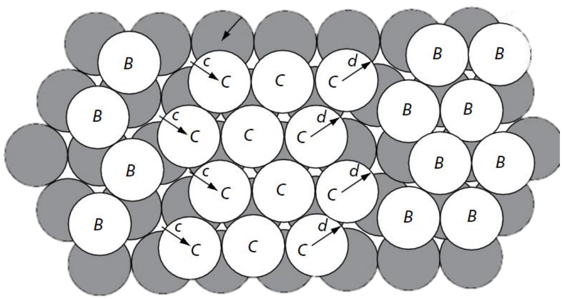

$$\boldsymbol{\Gamma} = 2\rho \boldsymbol{\Delta G^{\gamma \to \varepsilon}} + 2\sigma$$

$\boldsymbol{\Gamma}$: ***Stacking fault energy***

ρ : *molar surface density along* $\{111\}$ $\quad \rho = \frac{4}{\sqrt{3}} \frac{1}{a^2 N}$

$\Delta G^{\gamma \to \varepsilon}$: *Molar Gibbs energy of transformation*

σ : *Surface energy of interface* $(5 - 15\, mJ/m^{-2})$

Schokely Partial dislocation

$$\frac{1}{2}[\bar{1}10] = \frac{1}{6}[\bar{1}2\bar{1}] + \frac{1}{6}[\bar{2}11]$$

- Depending on the stacking fault energy, deformation mechanism of an alloy system can be changed from dislocation movement to phase transformation

$\Delta G^{\gamma \to \varepsilon}$ phase is the dominant factor to change the SFE of an alloy system

$Cr_{20}Mn_{20}Fe_{20}Co_{20}Ni_{20}$

Mn

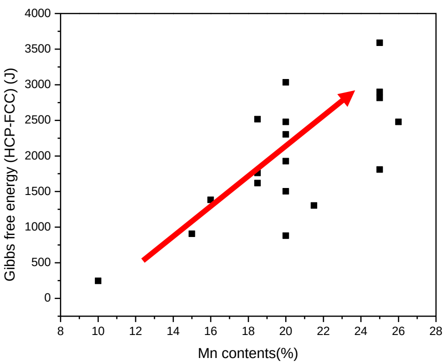

Ni

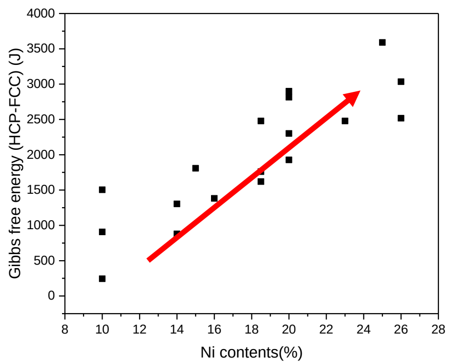

Fe

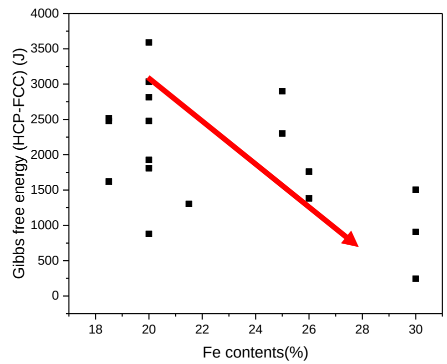

Co

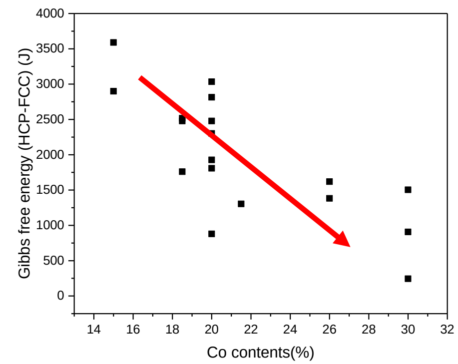

By Lowering $\Delta G^{\gamma\rightarrow\varepsilon}$, deformation mechanism can be changed

#	Composition	$\Delta G_{(hcp\text{-}fcc)}$(J)
1	$Cr_{20}Mn_{20}Fe_{20}Co_{20}Ni_{20}$	1927.8
2	$Cr_{20}Mn_{14}Fe_{24}Co_{24}Ni_{16}$	771.0
3	$Cr_{20}Mn_{10}Fe_{30}Co_{30}Ni_{10}$	245.3
4	$Cr_{20}Mn_{8}Fe_{32}Co_{32}Ni_{8}$	59.4

Confirmation of deformation mechanism through EBSD

undeform

	$Cr_{20}Mn_{20}Fe_{20}Co_{20}Ni_{20}$	$Cr_{20}Mn_{14}Fe_{26}Co_{26}Ni_{14}$	$Cr_{20}Mn_{10}Fe_{30}Co_{30}Ni_{10}$	$Cr_{20}Mn_{8}Fe_{32}Co_{32}Ni_{8}$
Bottom	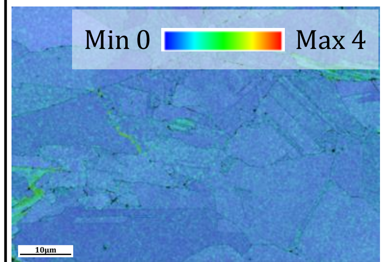	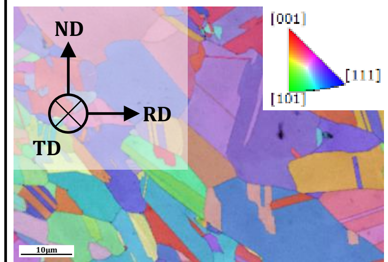		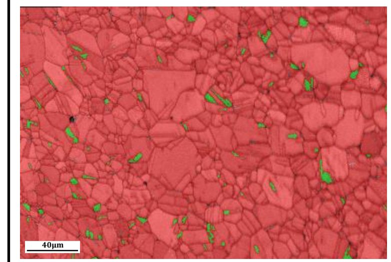
Bending	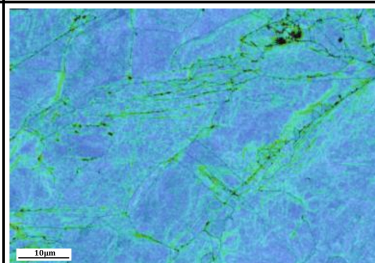	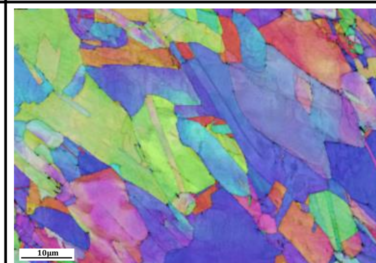	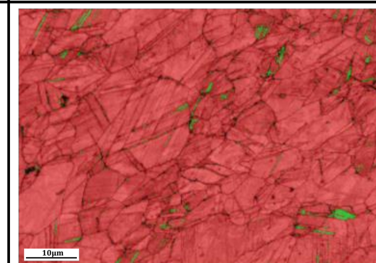	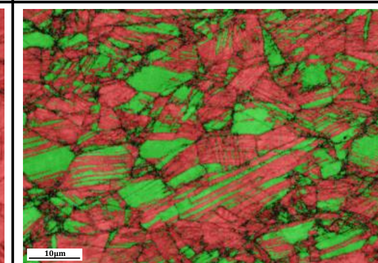
Dome	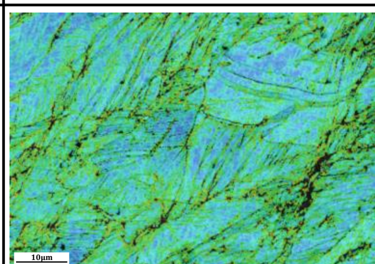	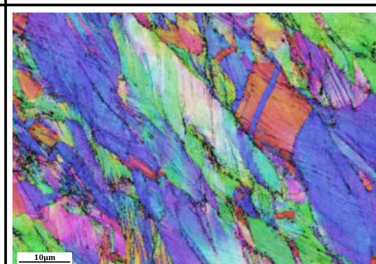	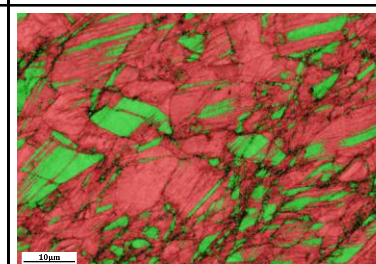	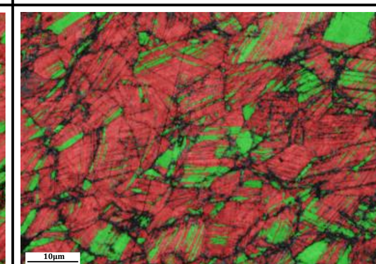
Dome Shape		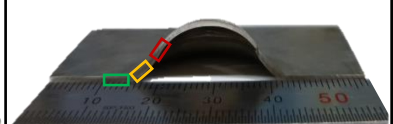	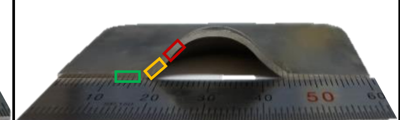	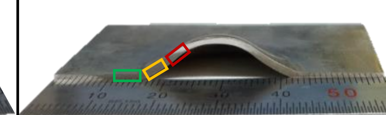
Note	**Cantor**	**TWIP**	**TRIP**	**TADP** (TRIP Assisted Dual Phase)

deform

Formability measurement method

Formability measurement method

Method 1

Forming Limit Diagram

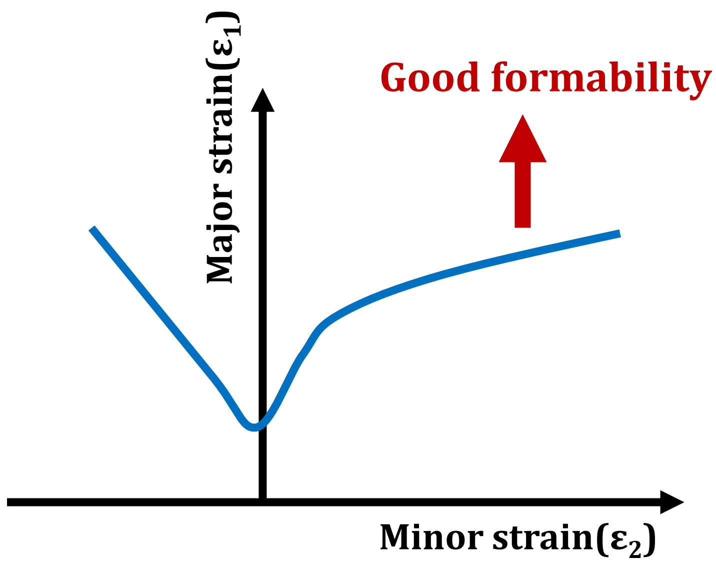

Reflect material's stretchability

Method 2

Limit Dome Height test

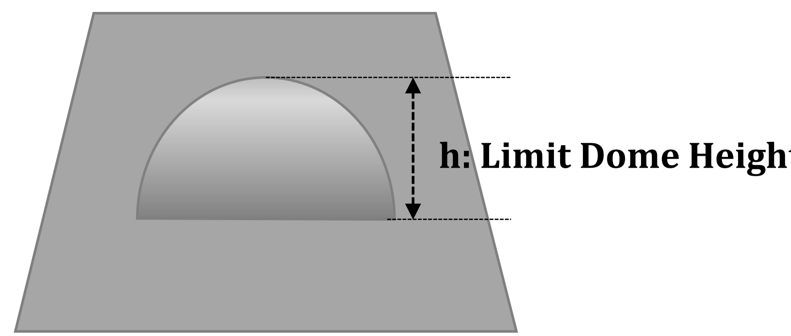

Limit Dome Height↑ : Good formability

Reflect material's drawability

S. P. Keeler, Met. Prog., October 1966, pp. 148-153

Before deformation of sheet

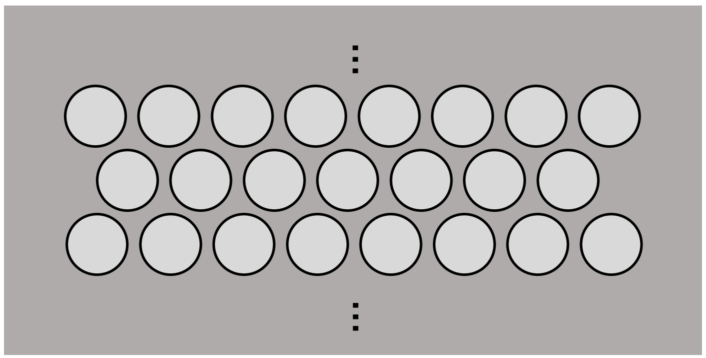

after deformation of sheet

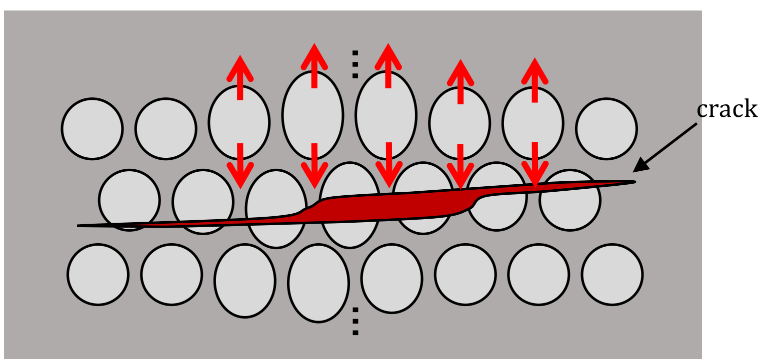

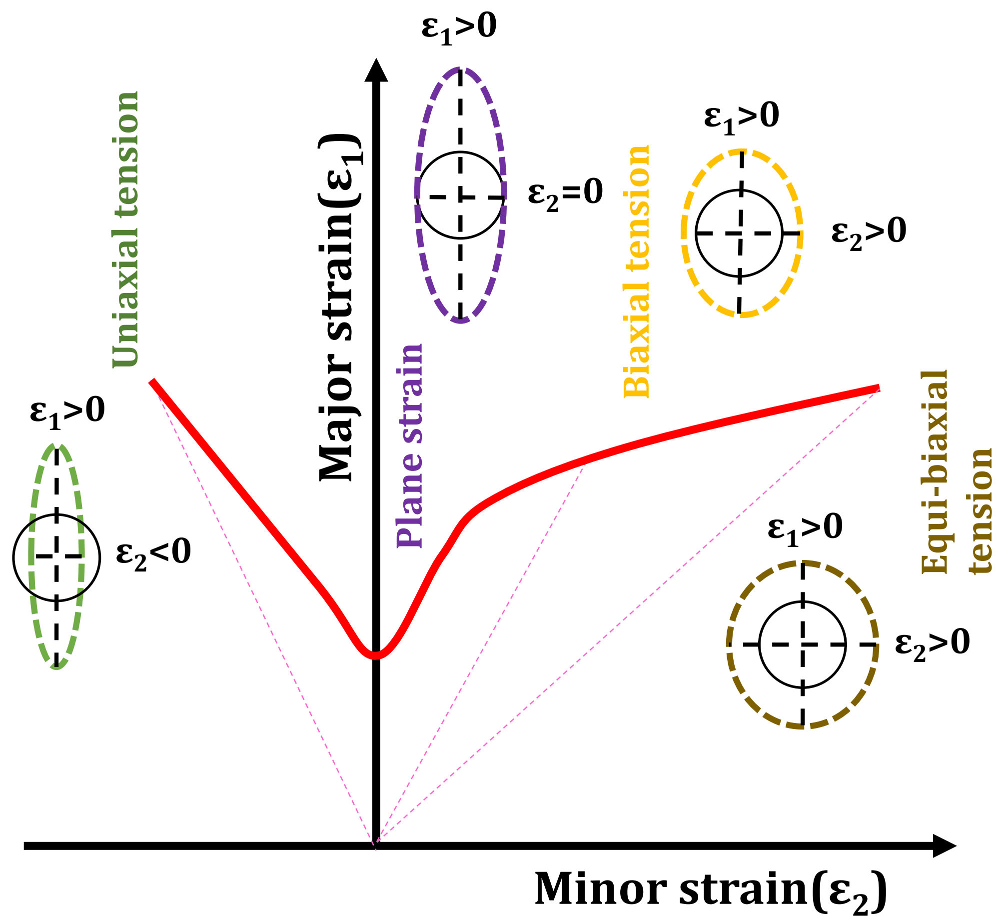

Formability *measurement method 1*: Forming Limit Diagram(Simulation)

K.S. Chung, M.G. Lee / Basics of Continuum Plasticity

Hardening law

- **Yield surface → Expansion**

- *Ludwick:* $\overline{\sigma} = \overline{\sigma}_y + K\overline{\varepsilon}^n$
- *Hollomon:* $\overline{\sigma} = K\overline{\varepsilon}^n$
- *Swift:* $\overline{\sigma} = K(\varepsilon_0 + \overline{\varepsilon})^n$
- *Voce:* $\overline{\sigma} = \overline{\sigma}_0 - exp\left(-n(\overline{\varepsilon} - \varepsilon_0)\right)$ ...

Isotropic hardening

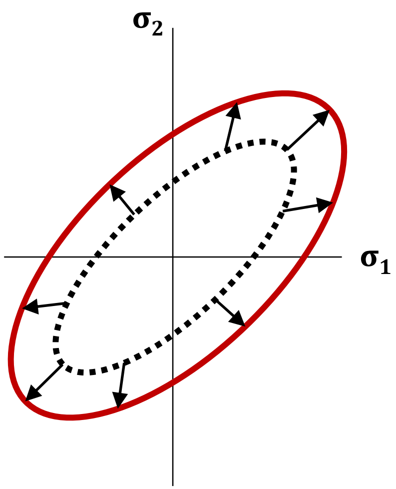

Kinetic hardening

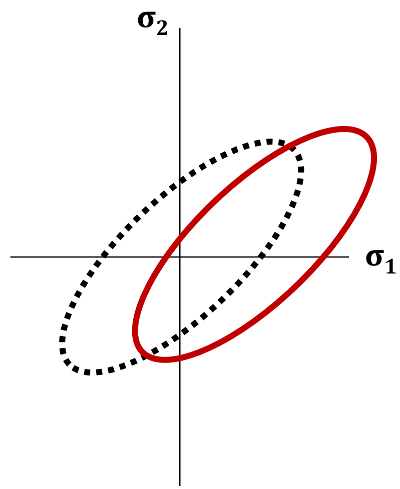

Combined isotropic Kinetic hardening

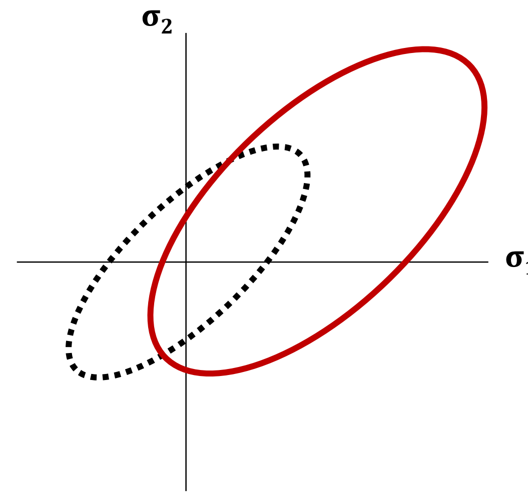

Yield criteria

- **Yield surface**

- *Von Mises*
- *Hill1948*
- *Yield2000*

...

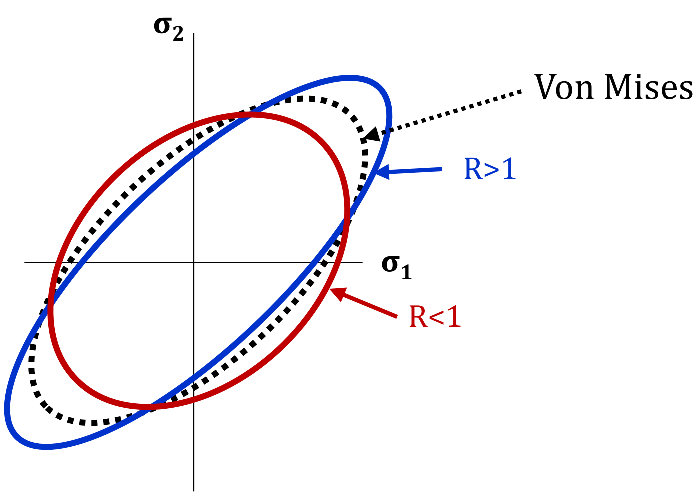

Hardening law, Yield criteria

↓ *M-K model*

Forming Limit Diagram

K.S. Chung, M.G. Lee / Basics of Continuum Plasticity

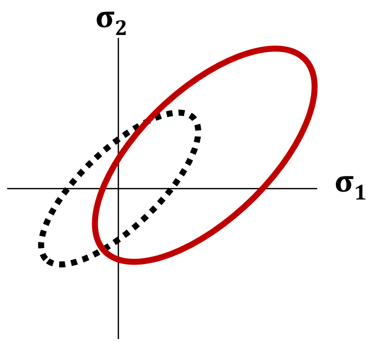

Hardening law

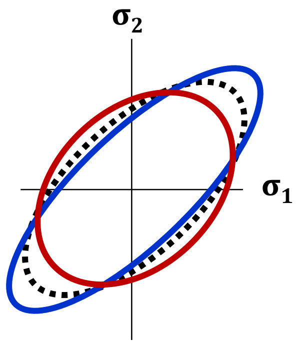

Yield criteria

Marciniak Kuczinsky(M-K) model → **Forming limit diagram**

Marciniak Kuczinsky(M-K) model

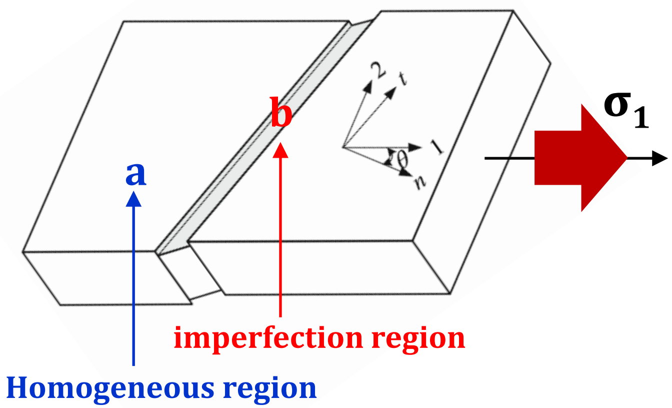

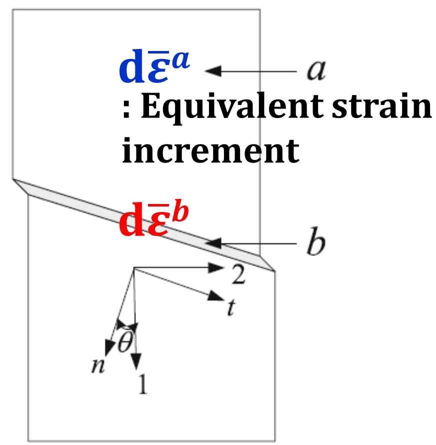

$$10d\bar{\varepsilon}^a \leq d\bar{\varepsilon}^b$$

: necking criterion is reached
→Computation is stopped

θ: initial defect in the form of narrow band inclined as an angle

M-K model is based on initial defect and assumes plastic localization occurs

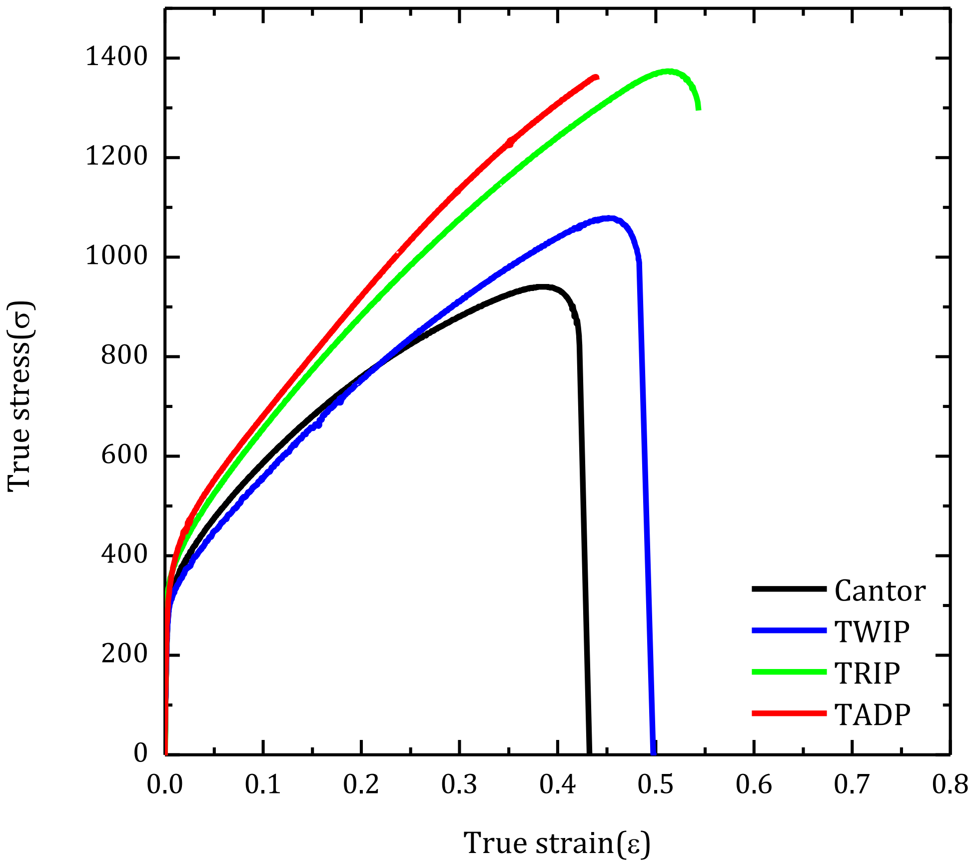

	Cantor	TWIP	TRIP	TADP
Yield stress(MPa)	307	279	291	300
Ultimate stress(MPa)	679	699	798	870
Uniform elongation	0.32	0.45	0.46	0.42
R-value	0.86	0.96	1.01	1.09

- **Uniform elongation ↑**

  Cantor < TADP < TWIP < TRIP

- **Strain hardening ↑**

  Cantor < TWIP < TRIP < TADP

TRIP and TADP are expected to have the good formability

Formability *measurement method 1*: Forming Limit Diagram

- **Material properties: 1) Uniaxial tensile test according to rolling direction (RD, TD, 45D)**

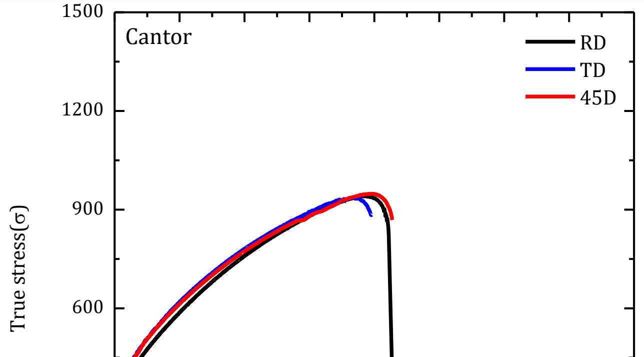

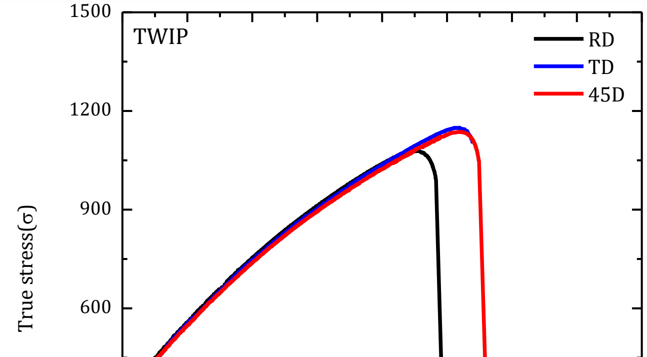

		Cantor	TWIP	TRIP	TADP
R-value	RD	0.88	0.94	1.02	1.07
	TD	0.94	0.97	1.02	1.08
	45D	1.02	0.97	1.03	1.07
Anisotropy factor (*R*)		**0.86**	**0.96**	**1.01**	**1.09**

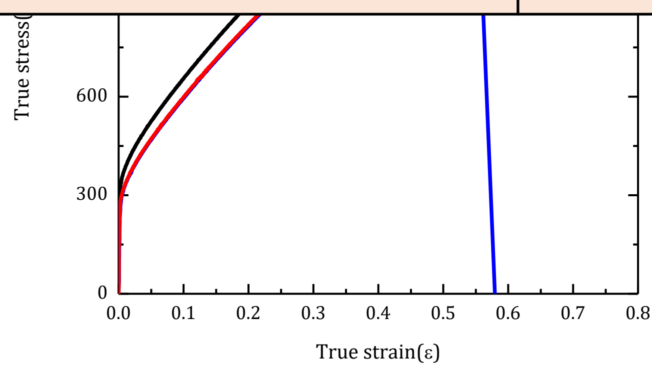

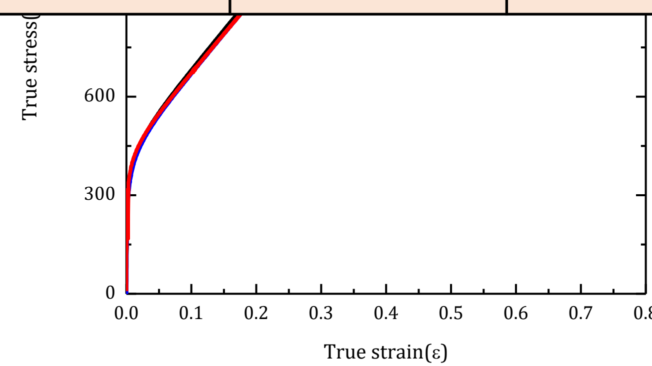

- **Material properties: 2) Hardening law**

- Thickness of specimen(mm) | Cantor : 1.38 / DP : 1.48 / TWIP : 1.38 / TRIP : 1.52
- Young's modulus E(GPa) | Cantor : 180.92 / DP : 180.00 / TWIP : 198.21 / TRIP : 188.02
- Poisson's ratio | Cantor : 0.25 / DP : 0.32 / TWIP : 0.28 / TRIP : 0.31
- Von Mises isotropic yield function
- Hardening law : Swift, Voce(better result)

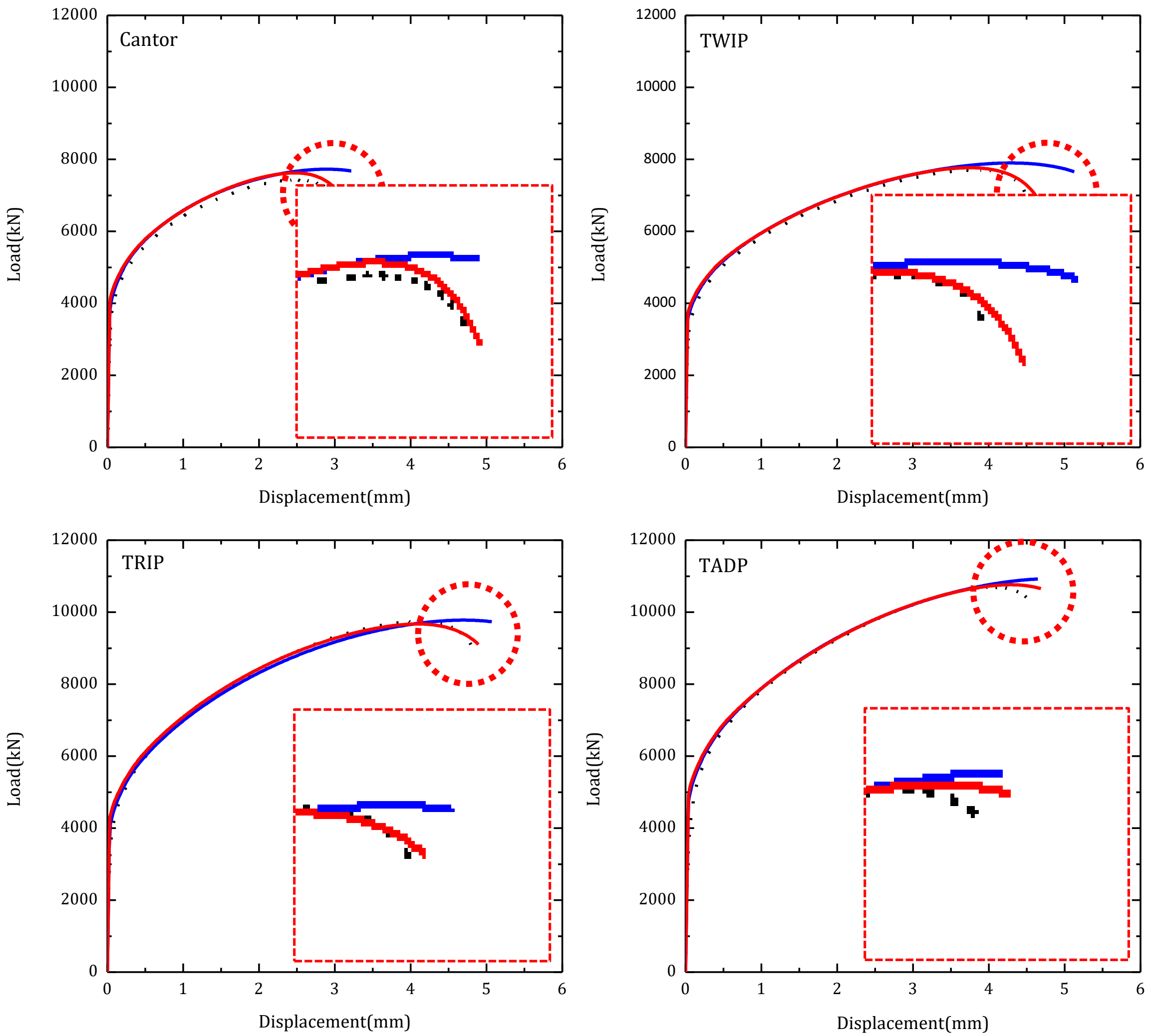

Swift hardening law $\bar{\sigma} = k(\bar{\varepsilon}_p + e_0)^n$

	k	e_0	n
Cantor	1462.31	0.0261	0.4077
TWIP	1632.66	0.0471	0.5479
TRIP	1892.71	0.0445	0.5770
TADP	2111.97	0.0564	0.6050

Voce hardening law $\bar{\sigma} = \sigma_0 + R(1 - e^{-b\bar{\varepsilon}_p})$

	σ_0	R	b
Cantor	355.67	793.36	4.1480
TWIP	322.91	1239.83	2.1954
TRIP	337.63	1587.39	1.9056
TADP	387.86	1850.02	1.7314

FE analysis result with Voce hardening law was chosen for further analysis

Formability *measurement method 1*: Forming Limit Diagram

- **Material properties: 3) Yield criteria**

1. Hill anisotropy: $F(\sigma_y - \sigma_z)^2 + G(\sigma_z - \sigma_x)^2 + H(\sigma_x - \sigma_y)^2 + 2L\tau_{yz}^2 + 2M\tau_{zx}^2 + 2N\tau_{zy}^2 = 1$

2. Yield 2000 criteria:

using measured R values

$$f^{\frac{1}{M}} = \{\frac{\emptyset}{2}\}^{\frac{1}{M}} = \bar{\sigma} \text{ with } \emptyset = \left|\widetilde{S1}' - \widetilde{S11}'\right|^M + \left|\widetilde{S11}' - \widetilde{S1}'\right|^M + \left|2\widetilde{S1}'' - \widetilde{S11}''\right|^M$$

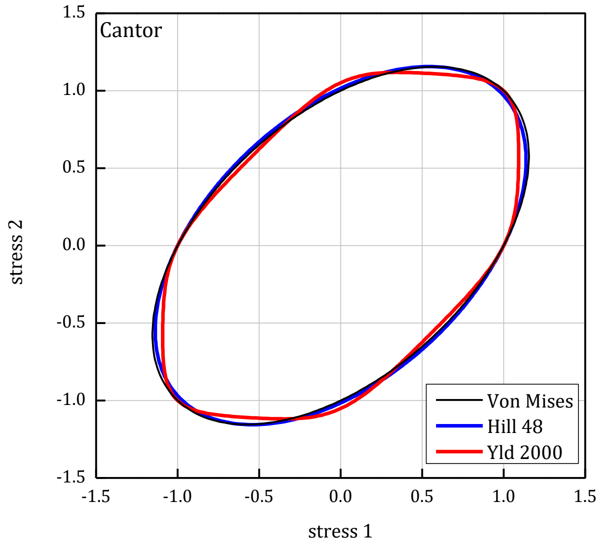

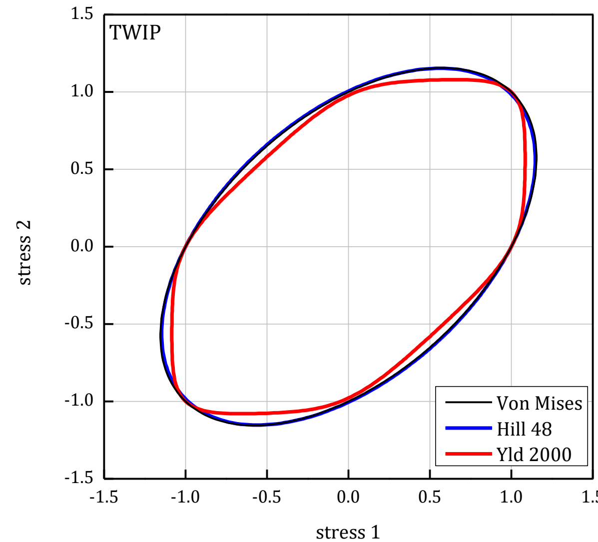

TWIP, TRIP TADP breaks rapidly after UTS

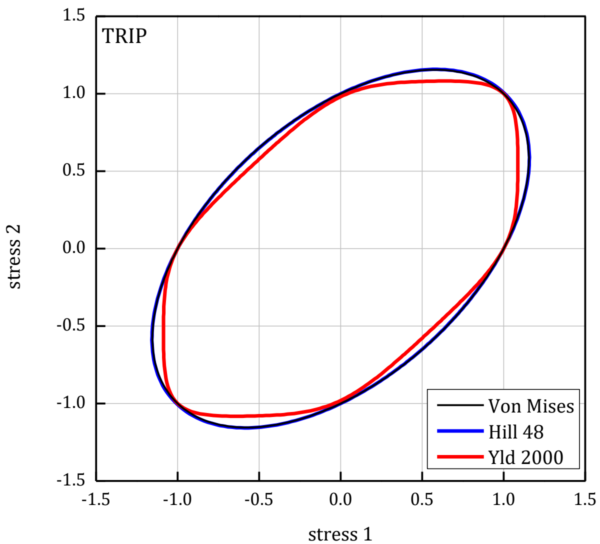

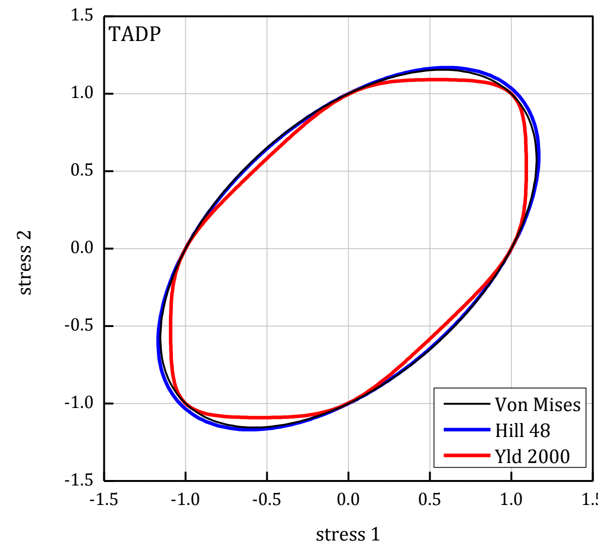

Yield 2000 criteria was chosen for further FEM simulation.

- **Material properties: Simulation factors**

- **hardening law: Voce**

$$\bar{\sigma} = \sigma_0 + R\left(1 - e^{-b\bar{\varepsilon}_p}\right) \quad \text{or } \bar{\sigma} = A - B exp(-C\bar{\varepsilon}), with\ B = \exp(n\varepsilon_0)$$

	Hardening law	A(S0)	B(R)	C(B)
Cantor	Voce	310	747.0954	5.516197
TWIP	Voce	322.9056	1239.834	2.195402
TRIP	Voce	337.6338	1587.389	1.905647
Dual Phase	Voce	387.8632	1850.025	1.731408

- **Yield function: Yield 2000**

	Yield function	A1	A2	A3	A4	A5	A6	A7	A8
Cantor	Yield 2000	1.044313	0.900592	1.063173	0.981113	0.997253	0.978494	0.986111	0.956883
TWIP	Yield 2000	0.964852	1.048262	0.969563	1.010907	1.004901	0.998649	1.014691	1.050405
TRIP	Yield 2000	0.975463	1.043968	0.975509	1.008013	1.002224	1.003852	1.003332	0.999599
Dual Phase	Yield 2000	1.000951	1.011217	1.001635	0.99864	0.997925	1.005233	1.007512	0.995052

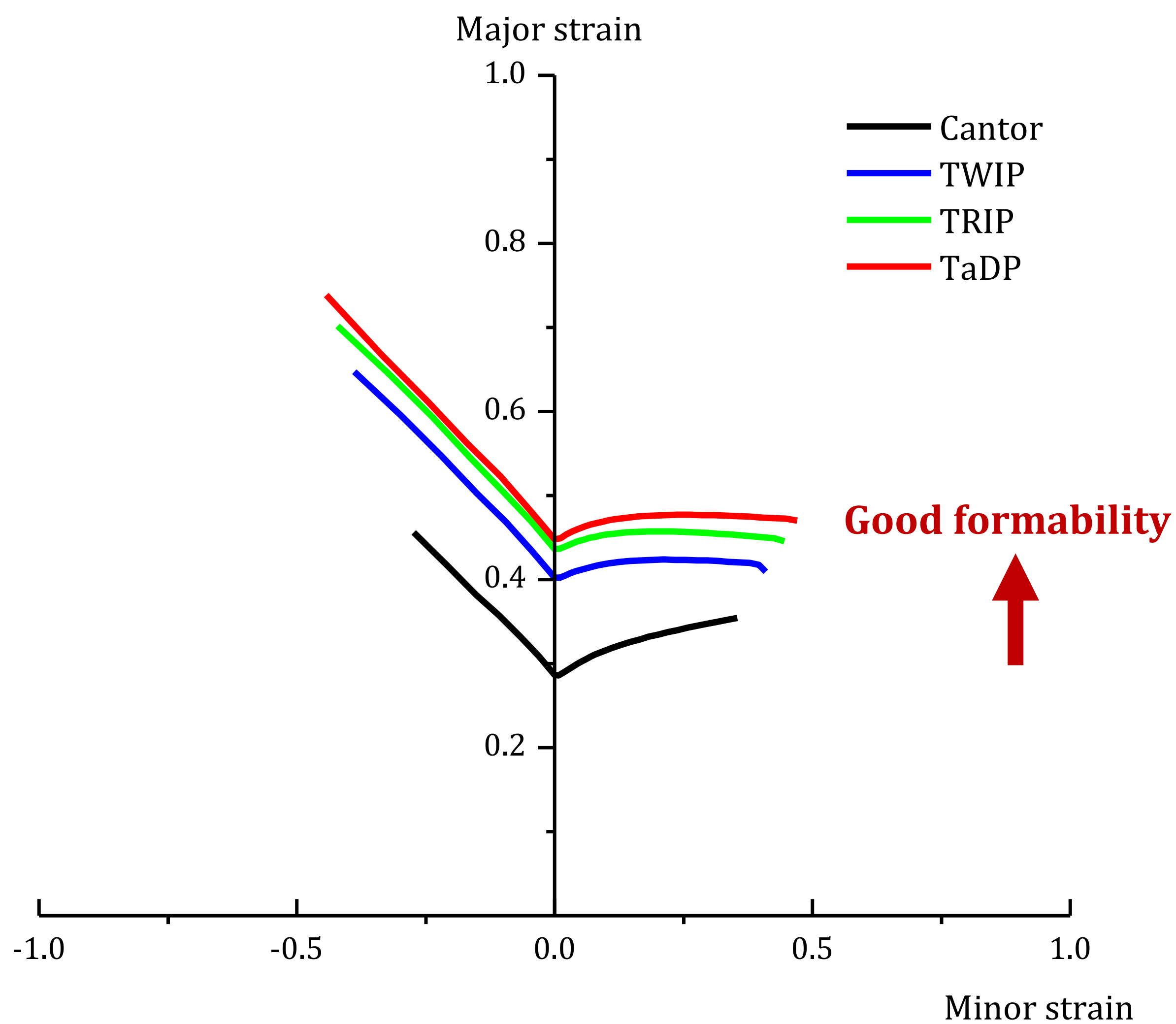

Forming Limit Diagram by Simulation : TADP > TRIP > TWIP > Cantor

Forming Limit Diagram of commercial alloys

[ref]
Fe18%MnAlC TWIP: De Cooman et al./ *State-of-the-knowledge on TWIP steel*
IF: De Cooman et al./ *State-of-the-knowledge on TWIP steel*
EDDQ: De Cooman et al./ *State-of-the-knowledge on TWIP steel*
Fe15%MnAlC TWIP: De Cooman et al./ *State-of-the-knowledge on TWIP steel*
TRIP 700: De Cooman et al./ *State-of-the-knowledge on TWIP steel*
5083 Al-Mg alloy: T. Naka et al./ *Journal of Material Processing Technology 113(2001) 648-653*
Ti6Al4V: F.Djavanroodi, A. Derogar/ *Materials and Design 31 (2010) 4866-4875*
Al6061-T6: F.Djavanroodi, A. Derogar/ *Materials and Design 31 (2010) 4866-4875*
Cantor: *experience*
TWIP: *experience*
TRIP: *experience*
Dual Phase: *experience*

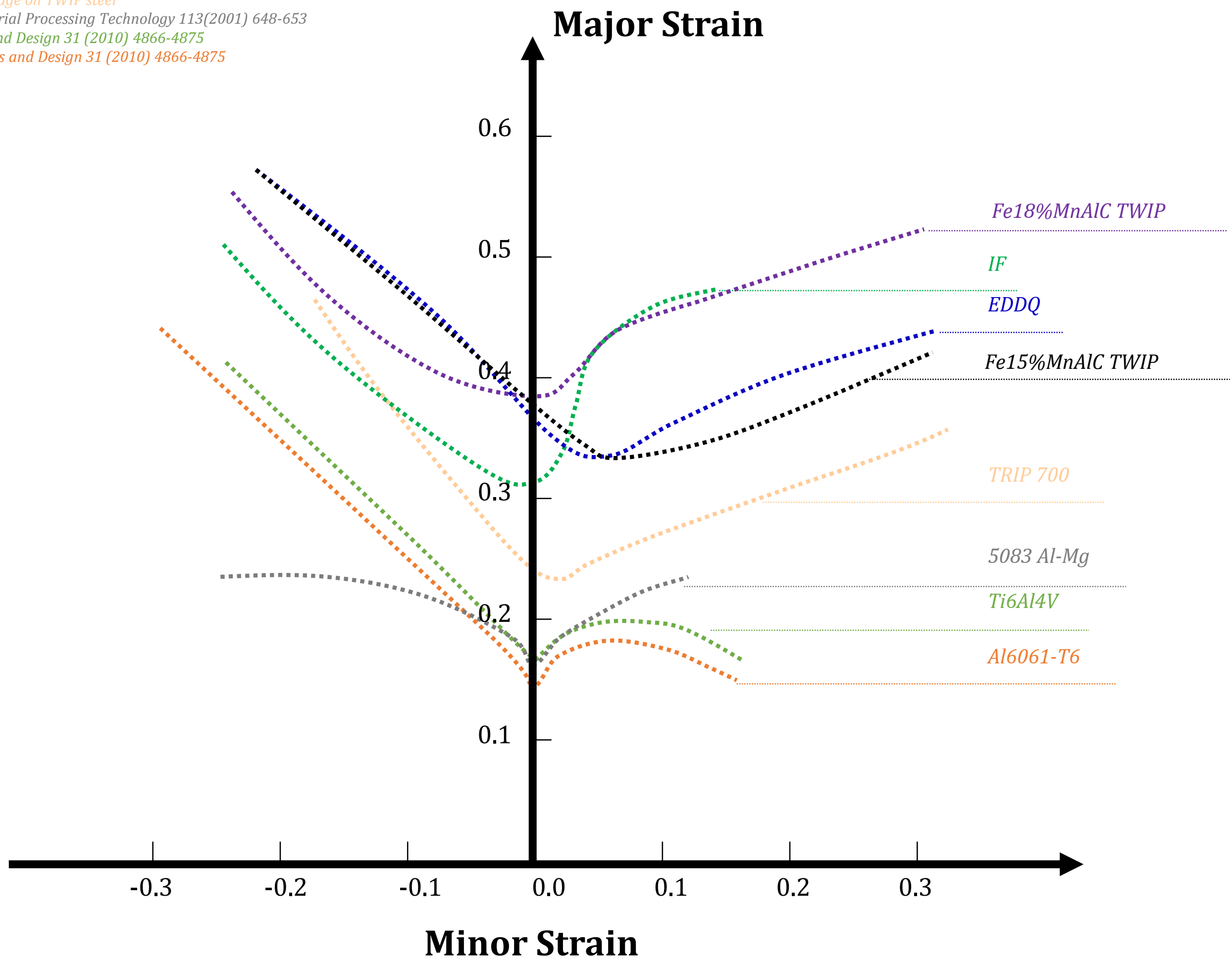

CCAs Forming Limit Diagram comparison with commercial alloys

[ref]
Fe18%MnAlC TWIP: De Cooman et al./ *State-of-the-knowledge on TWIP steel*
IF: De Cooman et al./ *State-of-the-knowledge on TWIP steel*
EDDQ: De Cooman et al./ *State-of-the-knowledge on TWIP steel*
Fe15%MnAlC TWIP: De Cooman et al./ *State-of-the-knowledge on TWIP steel*
TRIP 700: De Cooman et al./ *State-of-the-knowledge on TWIP steel*
5083 Al-Mg alloy: T. Naka et al./ *Journal of Material Processing Technology 113(2001) 648-653*
Ti6Al4V: F.Djavanroodi, A. Derogar/ *Materials and Design 31 (2010) 4866-4875*
Al6061-T6: F.Djavanroodi, A. Derogar/ *Materials and Design 31 (2010) 4866-4875*
Cantor: *experience*
TWIP: *experience*
TRIP: *experience*
Dual Phase: *experience*

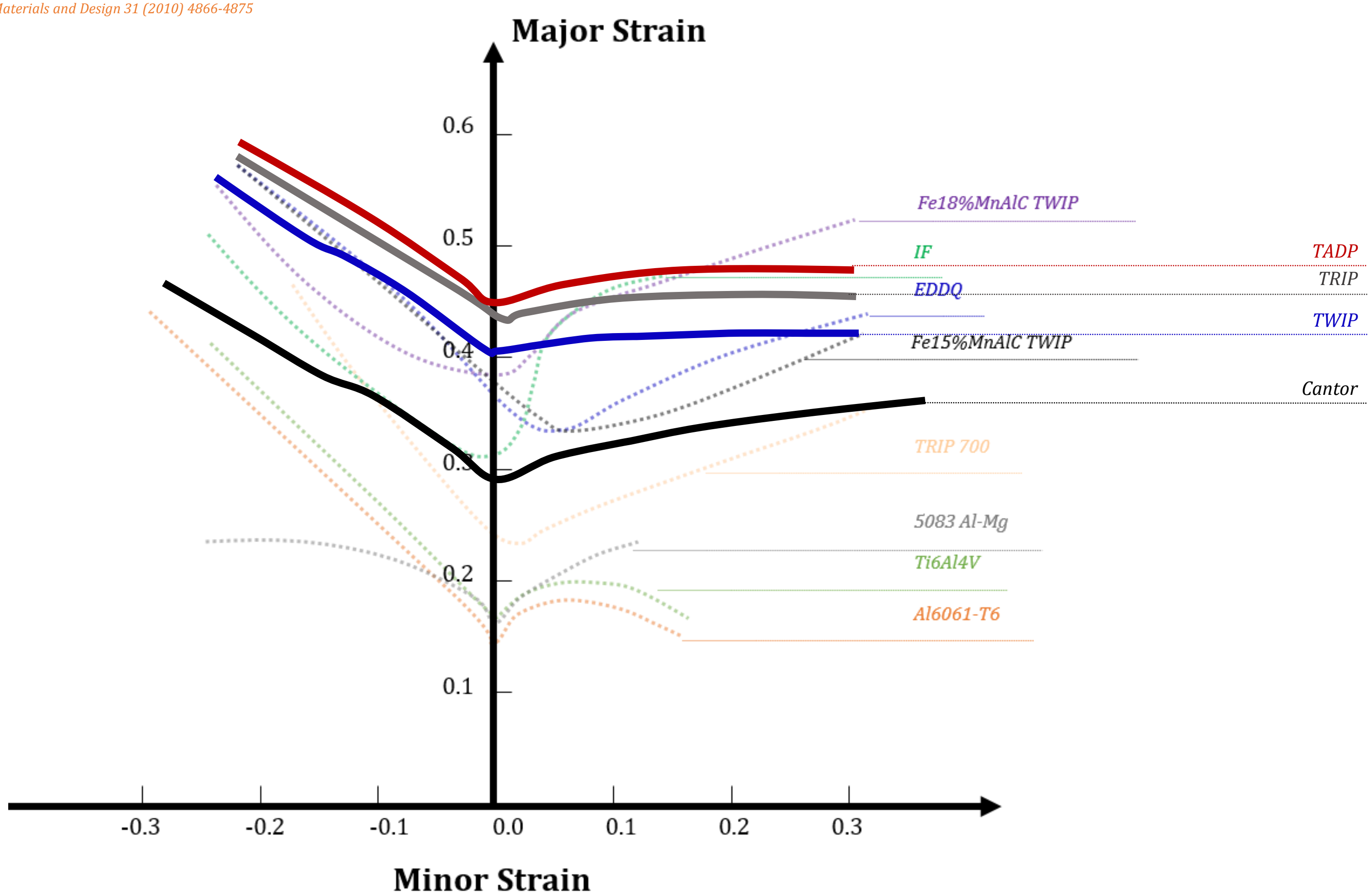

Cantor

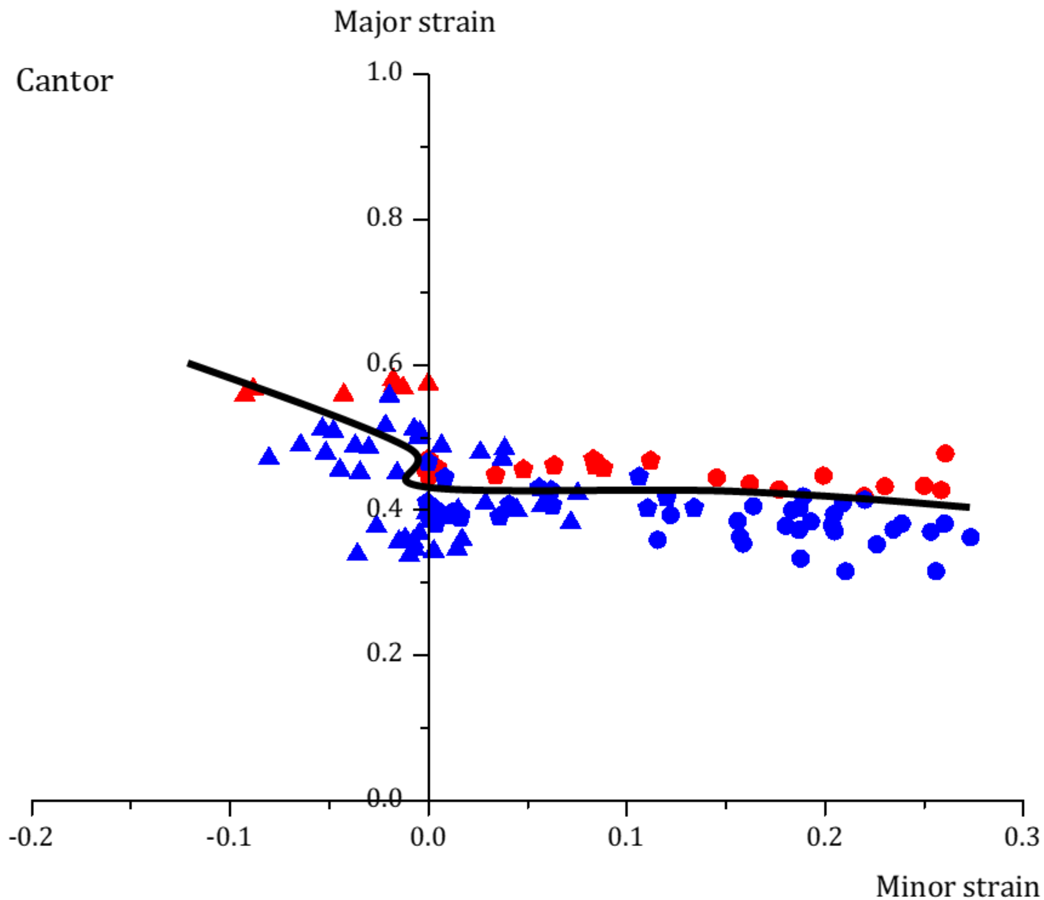
Major strain
Cantor
1.0
0.8
0.6
0.4
0.2
0.0
-0.2
-0.1
0.0
0.1
0.2
0.3
Minor strain

Formability measurement method 1: Forming Limit Diagram(Experiment)

TWIP

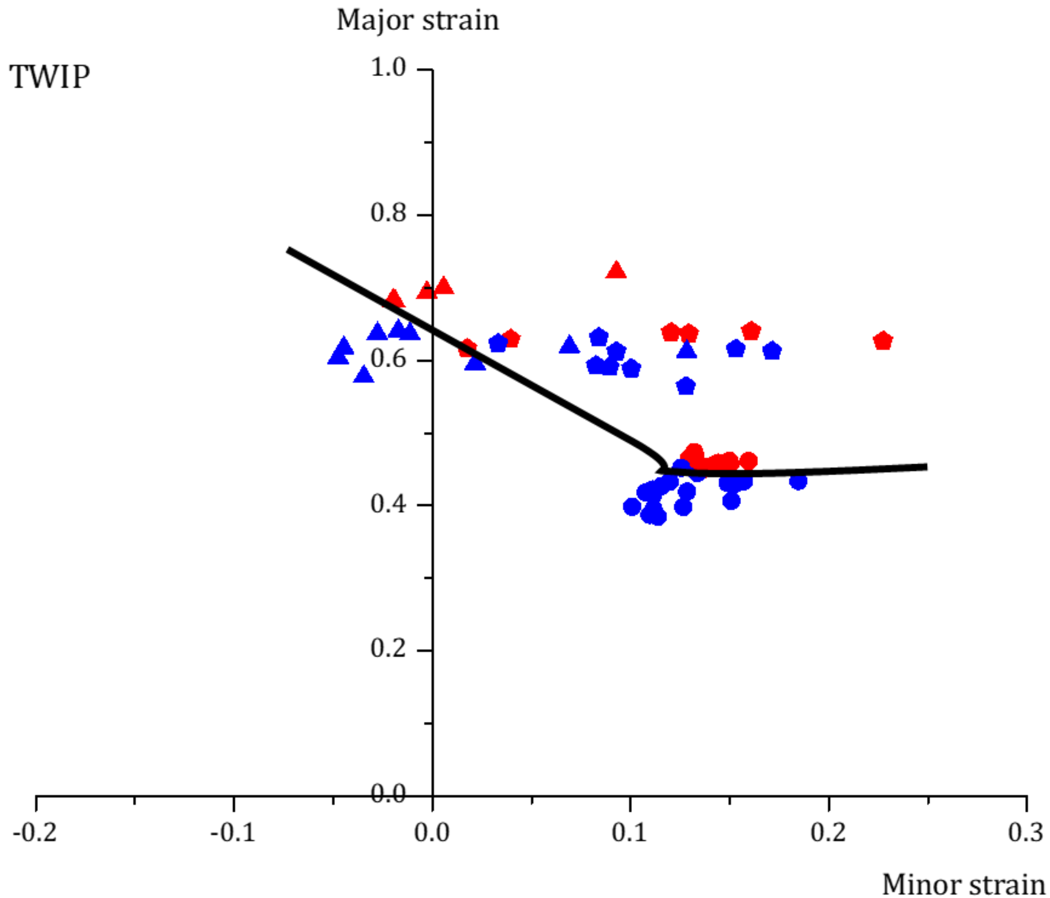

TRIP

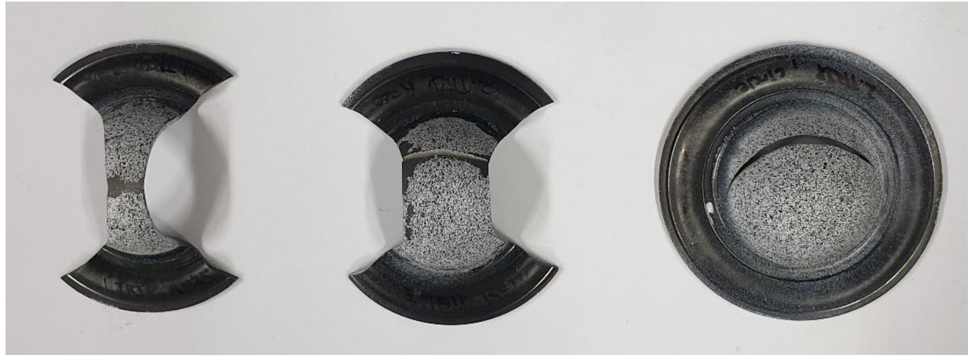

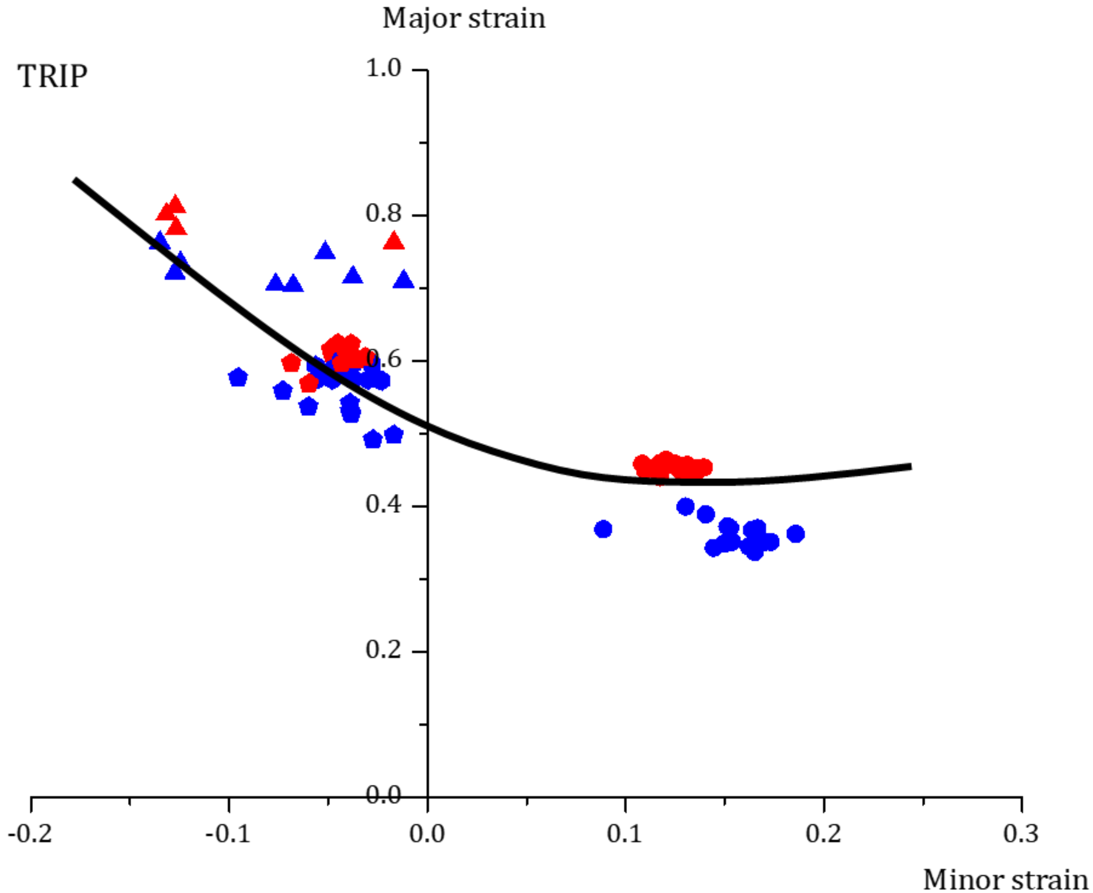

Major strain
TRIP
1.0
0.8
0.6
0.4
0.2
0.0
-0.2
-0.1
0.0
0.1
0.2
0.3
Minor strain

TADP

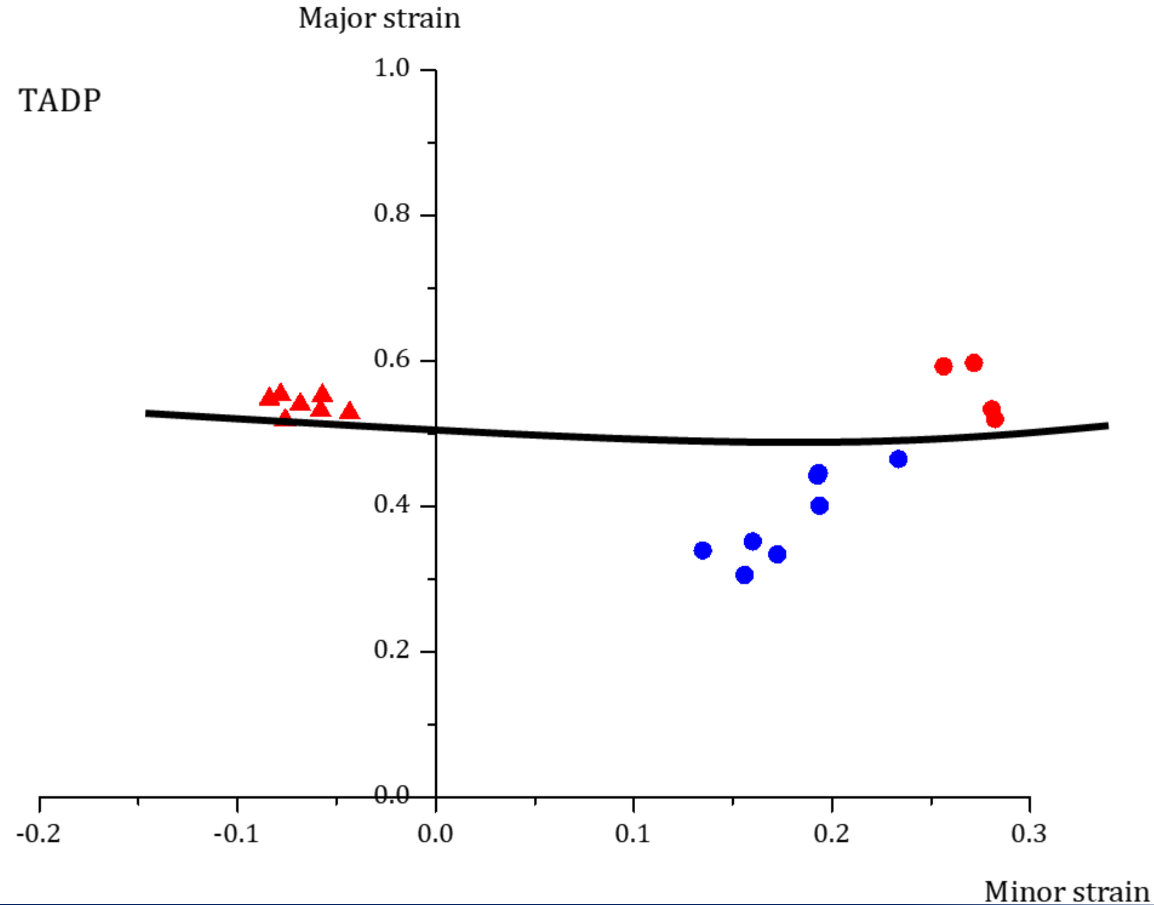
Major strain
TADP
1.0
0.8
0.6
0.4
0.2
0.0
-0.2
-0.1
0.0
0.1
0.2
0.3
Minor strain

Formability measurement method 1: Forming Limit Diagram(Experiment)

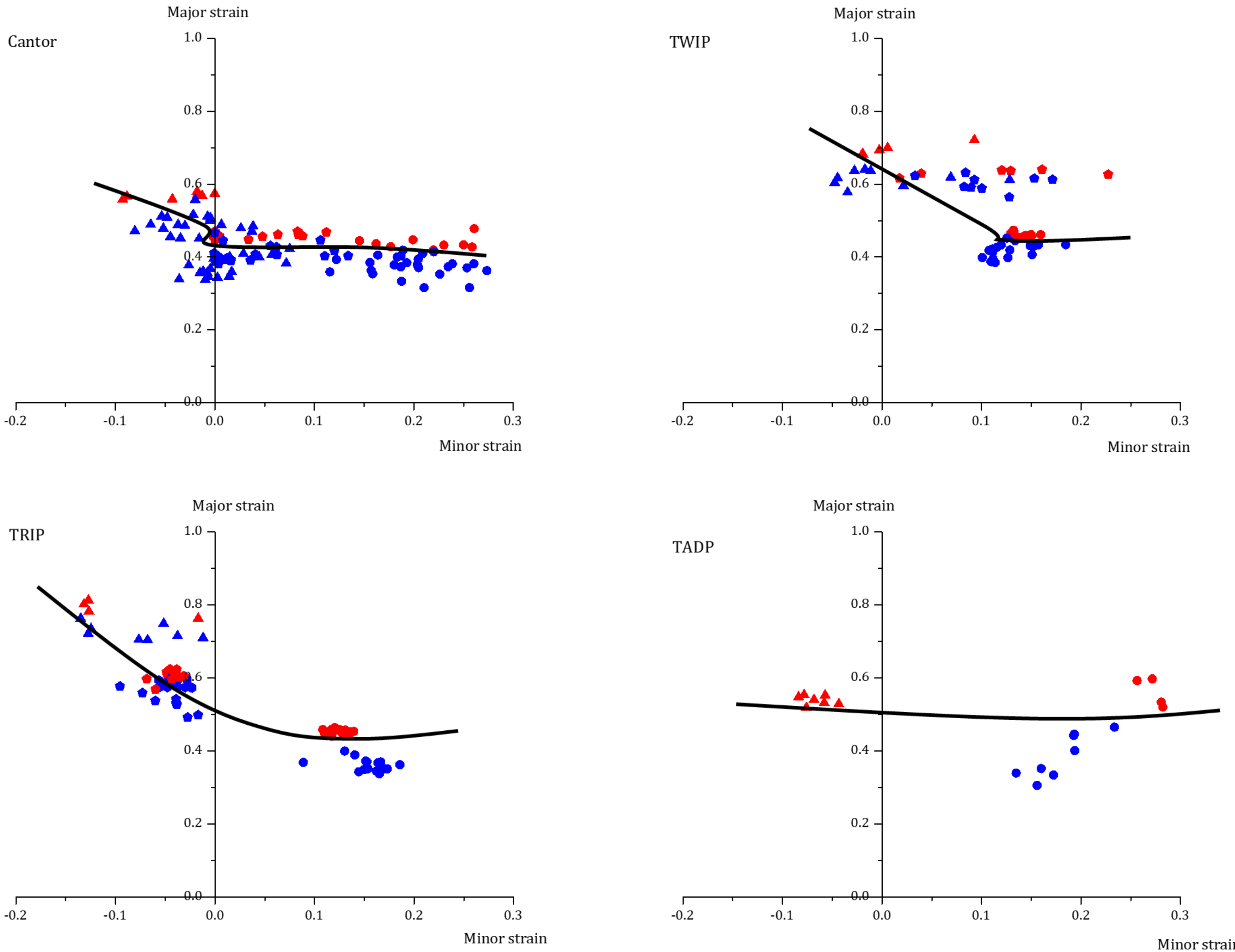

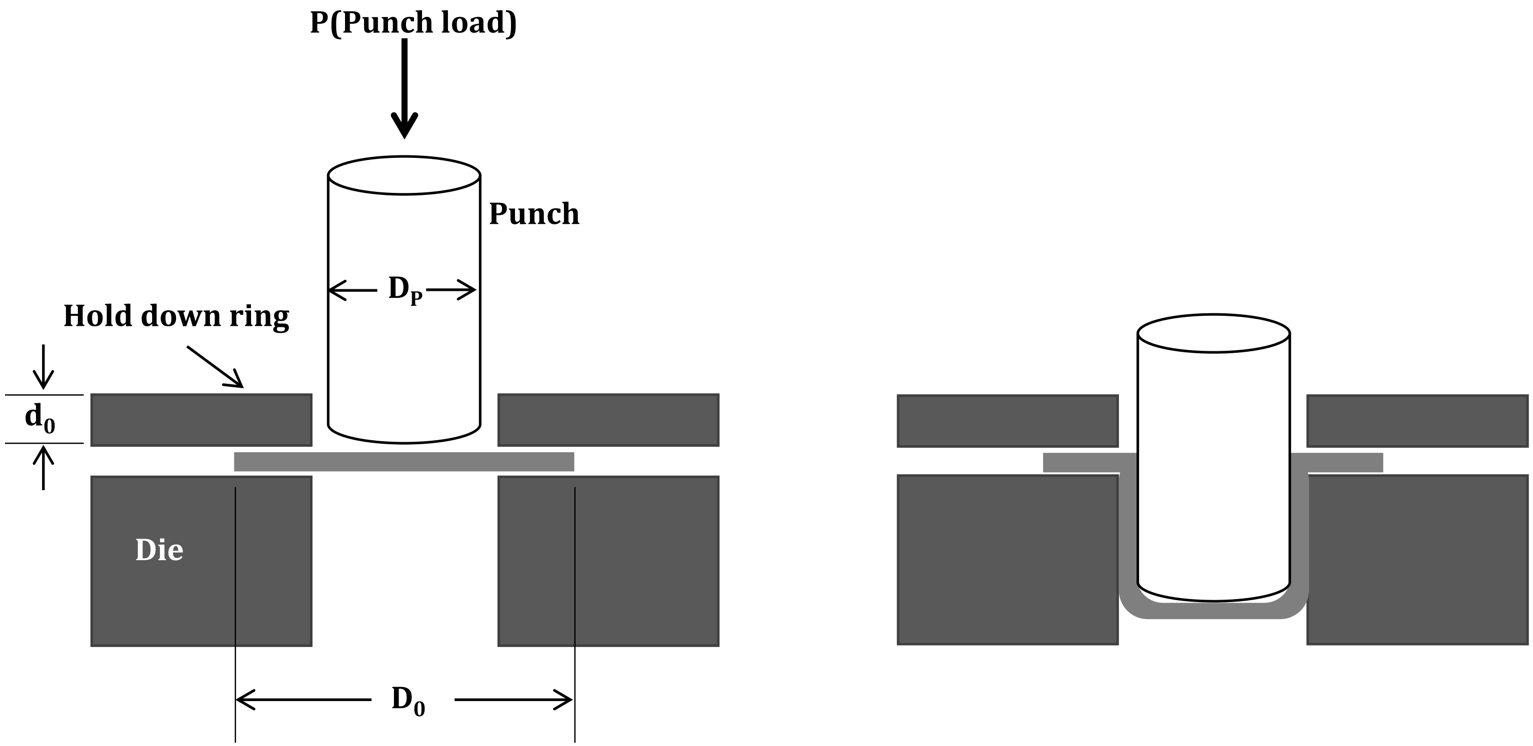

Before punching

After punching

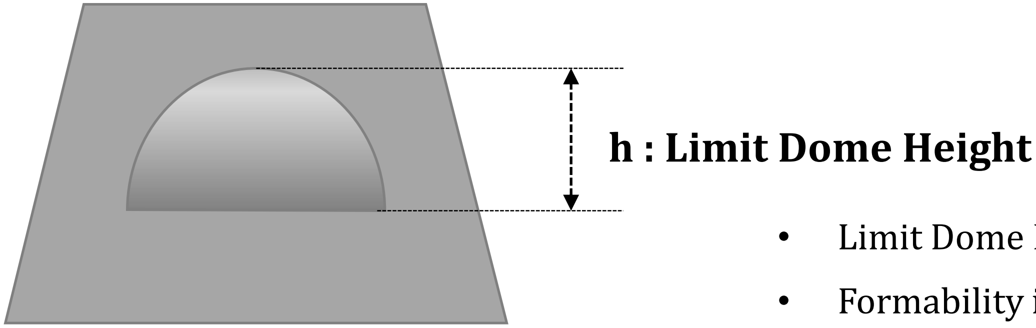

- Limit Dome Height is stopped right after fracture occur
- Formability is evaluated by Limit Dome Height value

Formability is determined by relative value of Limit Dome Height

Formability *measurement method 2*: Limit Dome Height test

- **Specimen preparation**

RD →

Cantor **TWIP** **TRIP** **TADP**

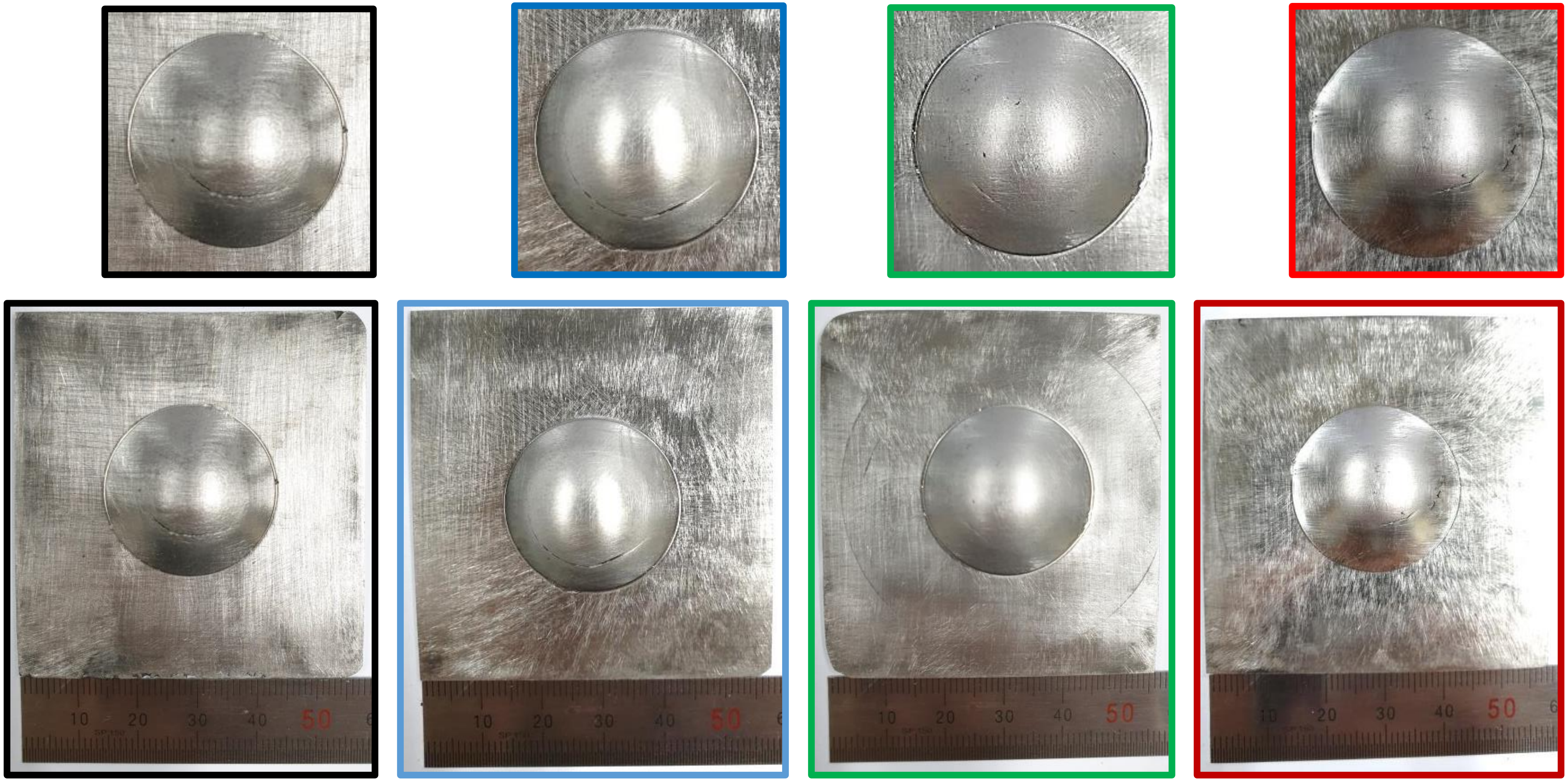

Limit Dome Height(LDH) test is stopped right after fracture occur

Results(*measurement method 2*): Limit Dome Height test

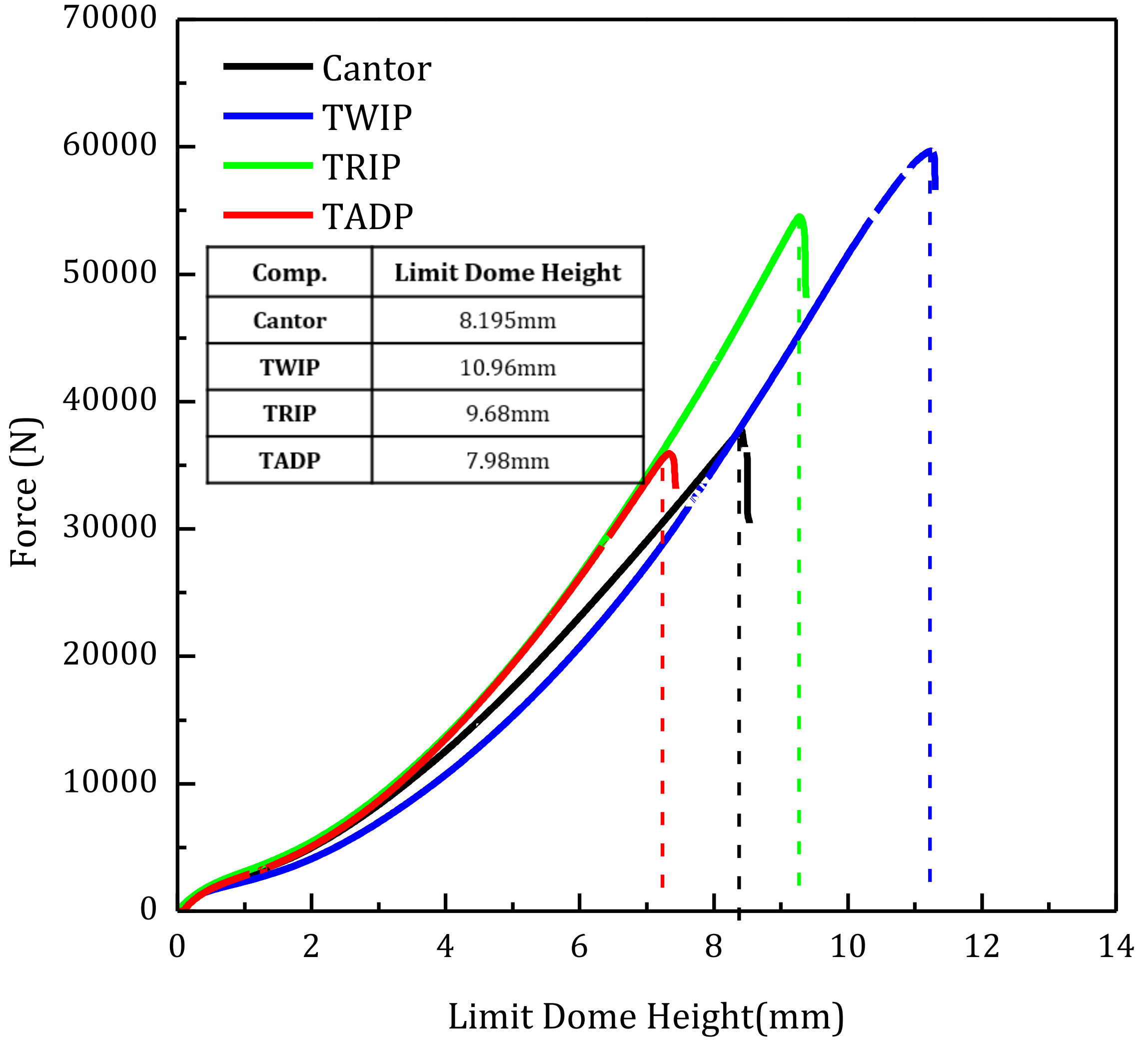

Comp.	Limit Dome Height
Cantor	8.195mm
TWIP	10.96mm
TRIP	9.68mm
TADP	7.98mm

Good formability

TWIP(10.95mm)>TRIP(9.68mm)>Cantor(8.195mm)>TADP(7.98mm)

Comparison uniaxial Tensile test and Limit Dome Height Test

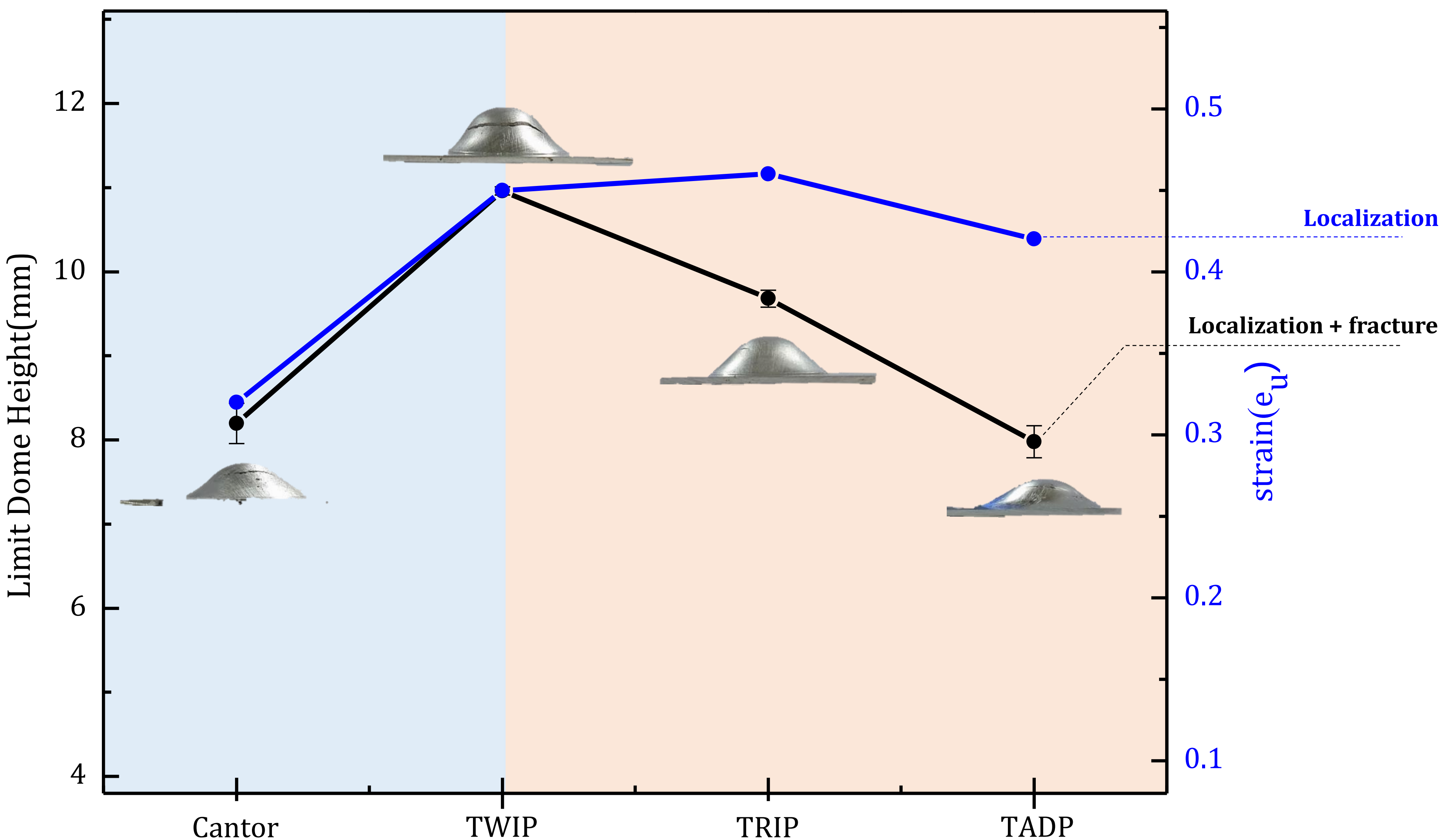

$$\text{Triaxiality}(\eta) = \frac{\sigma_m}{\sigma_{eq}} = \frac{\frac{1}{3}(\sigma_1+\sigma_2+\sigma_3)}{\frac{1}{\sqrt{2}}\sqrt{(\sigma_1-\sigma_2)^2+(\sigma_2-\sigma_3)^2+(\sigma_3-\sigma_1)^2+6[(\sigma_{12})^2+(\sigma_{23})^2+(\sigma_{13})^2]}}$$

σ_m = hydrostatic stress

σ_{eq} = von Mises equivalent stress

Stress triaxiality (η) represented stress state by the scalar value

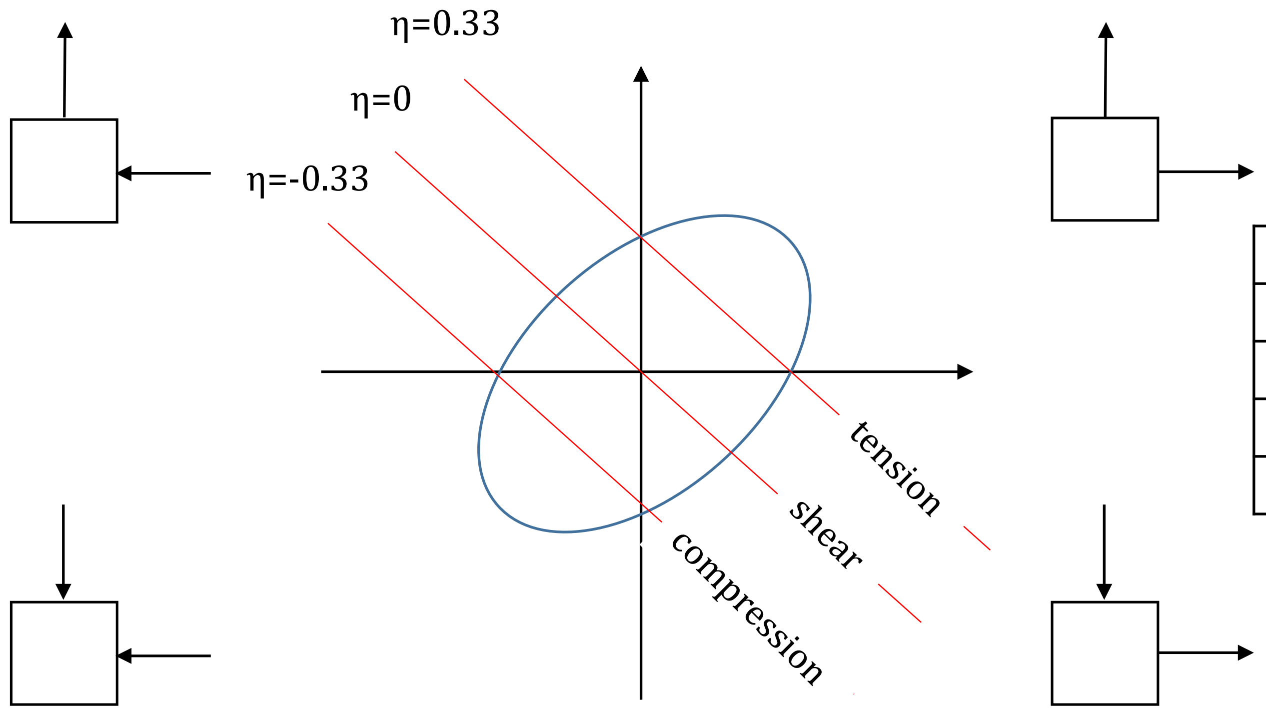

Stress state	η
Uniaxial tension	0.33
Equi-biaxial tension	0.67
Plane strain tension	0.58
Simple shear	0

By changing the triaxiality, the stress state applied to the material can be adjusted

Fracture test: Example of specimen(2024 Aluminum alloy)

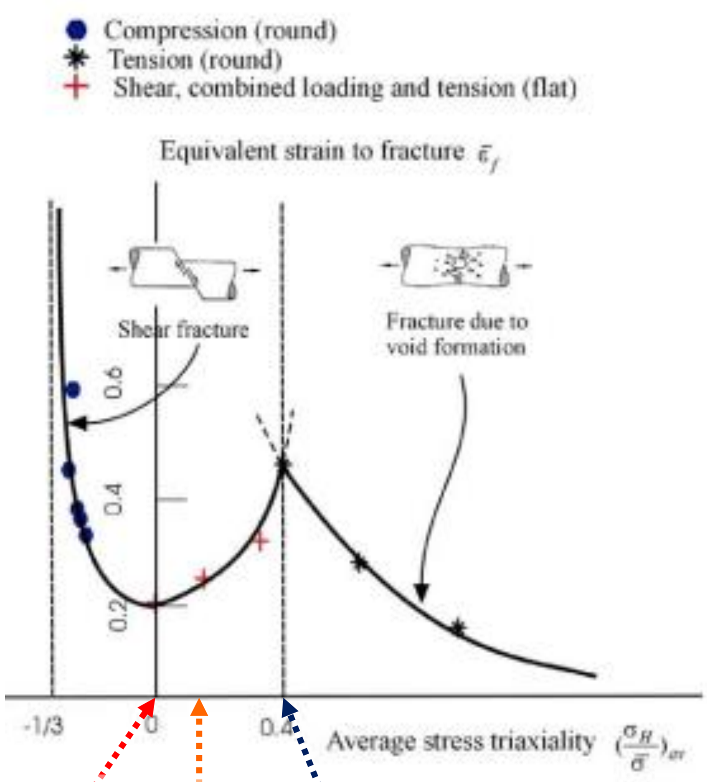

Pure shear test

Uniaxial tension

Shear+tension

International Journal of Mechanical Science 46 (2004) 81-98

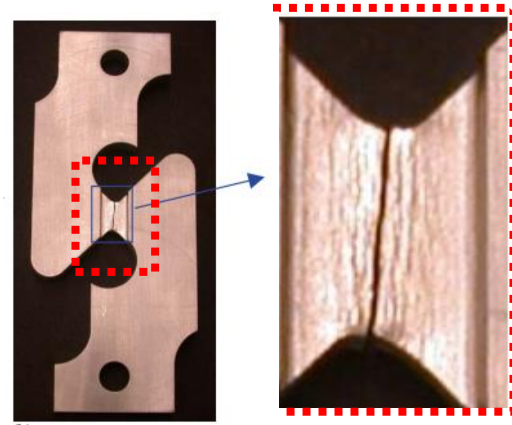

Pure shear

- Triaxiality: 0 ~ 0.02

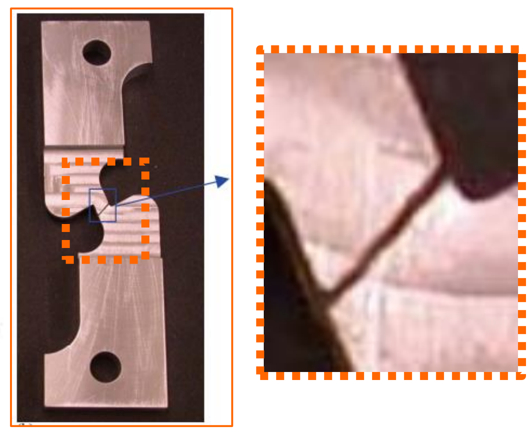

Combined shear & tension

- Triaxiality: 0.04 ~ 0.15

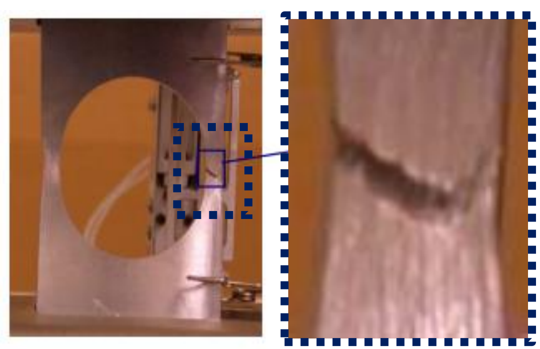

Circular hole (tensile loading)

- Triaxiality: 0.33

FE model

- Software : abaqus/standard
- Quarter symmetry model
- Element type :
  8node brick element with reduced integration (C3D8R)
- Element size at critical point :
  0.05mm x 0.05mm x (thickness/16)
- Number of element :
  CH – 14672 / NT – 17632
- Number of node :
  CH – 16853 / NT – 20032

$$\textbf{Triaxiality}(\eta) = \frac{\sigma_m}{\sigma_{eq}}$$

$$= \frac{\frac{1}{3}(\sigma_1+\sigma_2+\sigma_3)}{\frac{1}{\sqrt{2}}\sqrt{(\sigma_1-\sigma_2)^2+(\sigma_2-\sigma_3)^2+(\sigma_3-\sigma_1)^2+6[(\sigma_{12})^2+(\sigma_{23})^2+(\sigma_{13})^2]}}$$

- **Central hole**

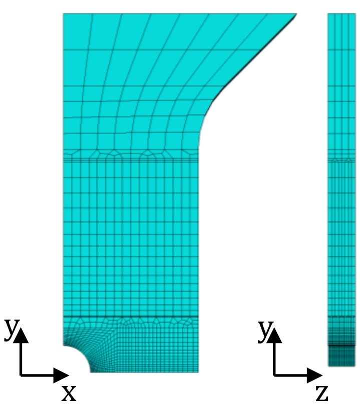

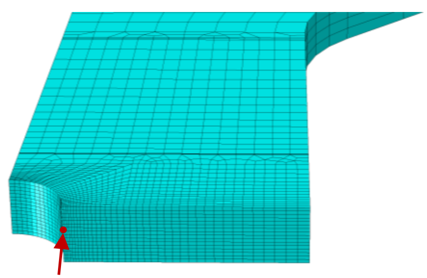

Critical point, stress and strain history is obtained at here

→ uniaxial stress state

- **Notched test**

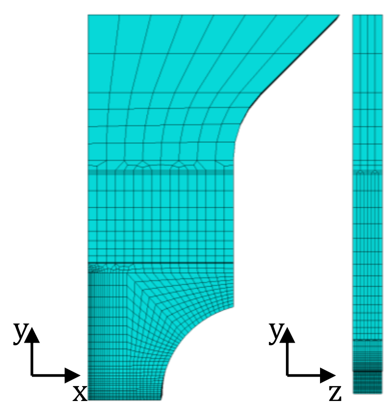

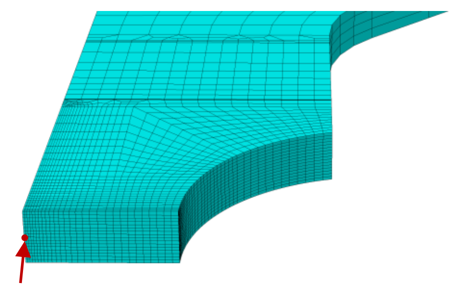

Critical point, stress and strain history is obtained at here

→ plane stress state

Fracture test: Experimental setup

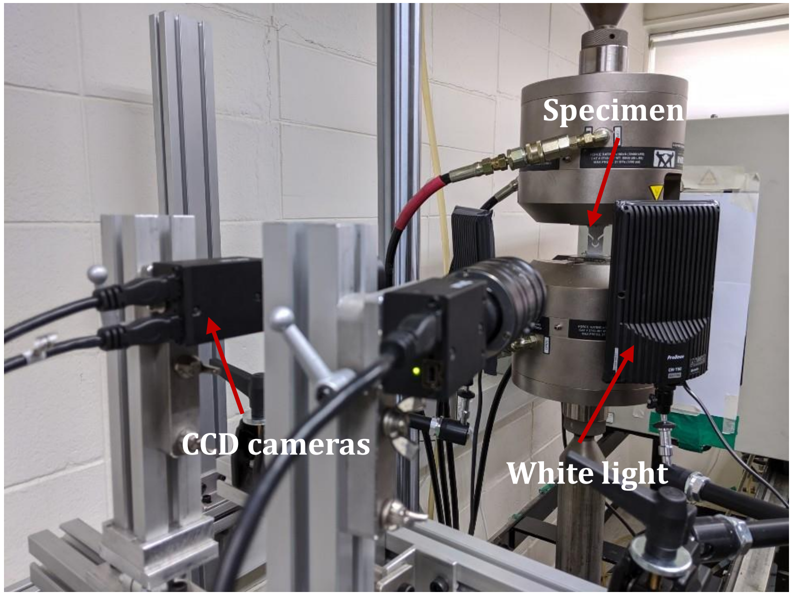

Mechanical test conditions	
Frame	Instron 8801
Load cell capacity	100kN
Test speed	1mm/min

DIC conditions	
DIC type : Stereo DIC	
Software	VIC-3D 7
CCD resolution (pixcels)	2448 x 2048
CCD sensor	2/3 inch grey scale

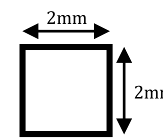

- **Central hole**

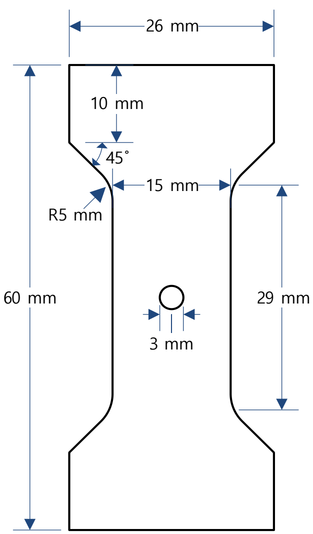

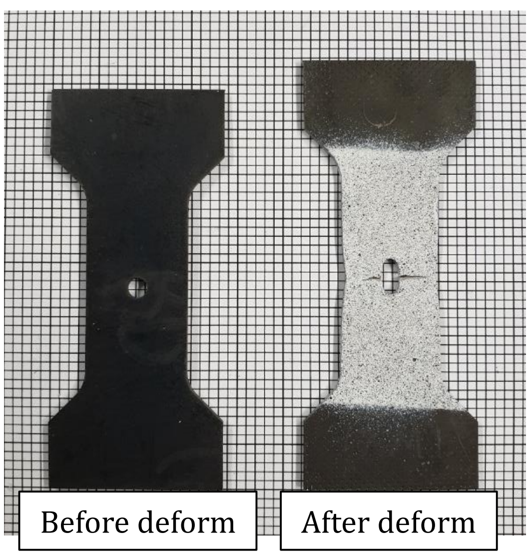

- **Notched test**

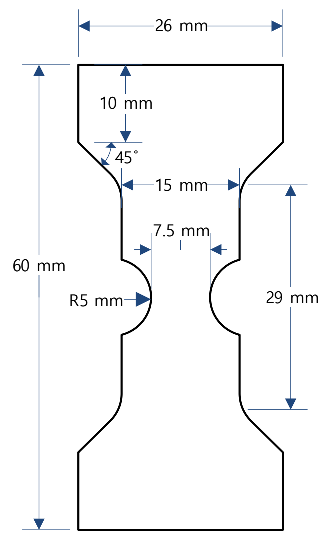

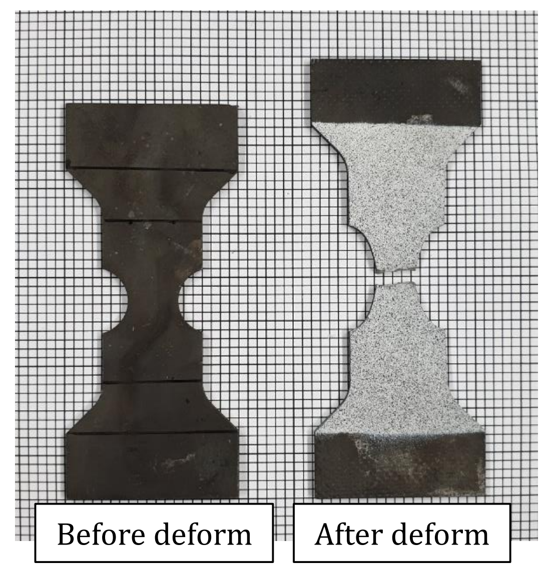

FE analysis of η of Central hole test: uniaxial stress state

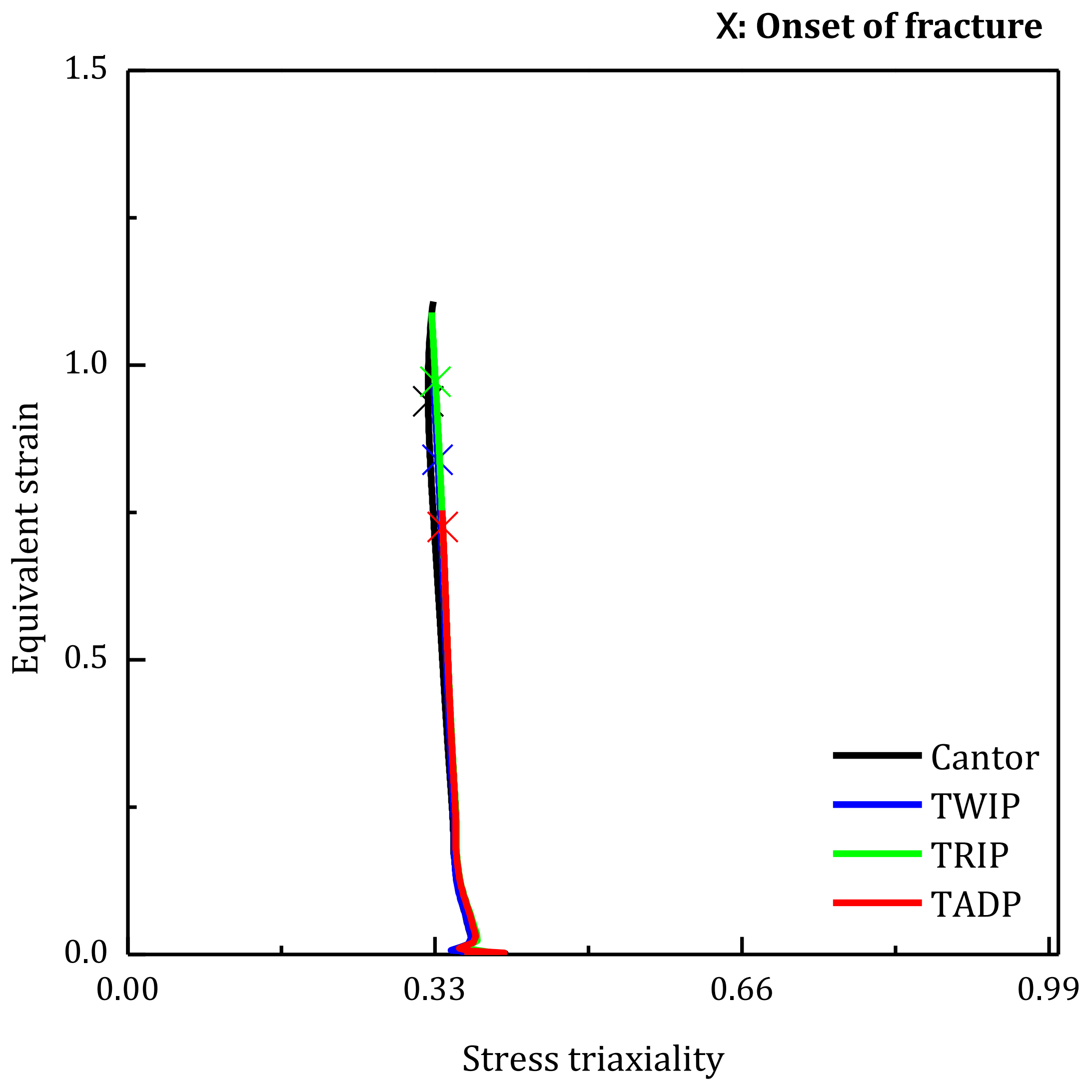

With increasing equivalent strain, stress triaxiality (η)=0.33 is maintained in Central hole test

FE analysis of η of Notched test: uni - biaxial stress state

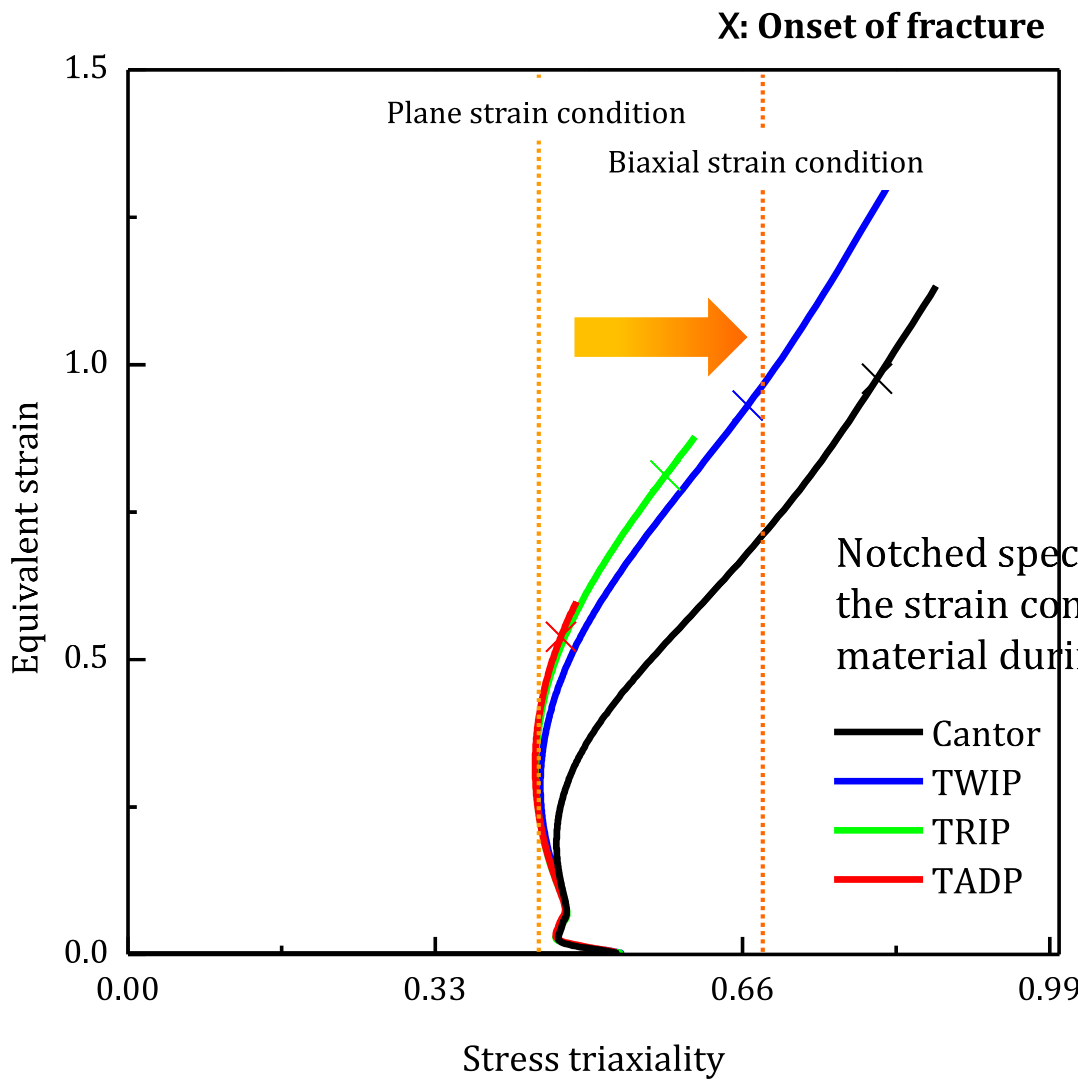

Notched specimen reflects the strain condition of the material during deformation.

With increasing equivalent strain, η changes from 0.56 to 0.66

Comparison of Central hole and Notched test equivalent strain

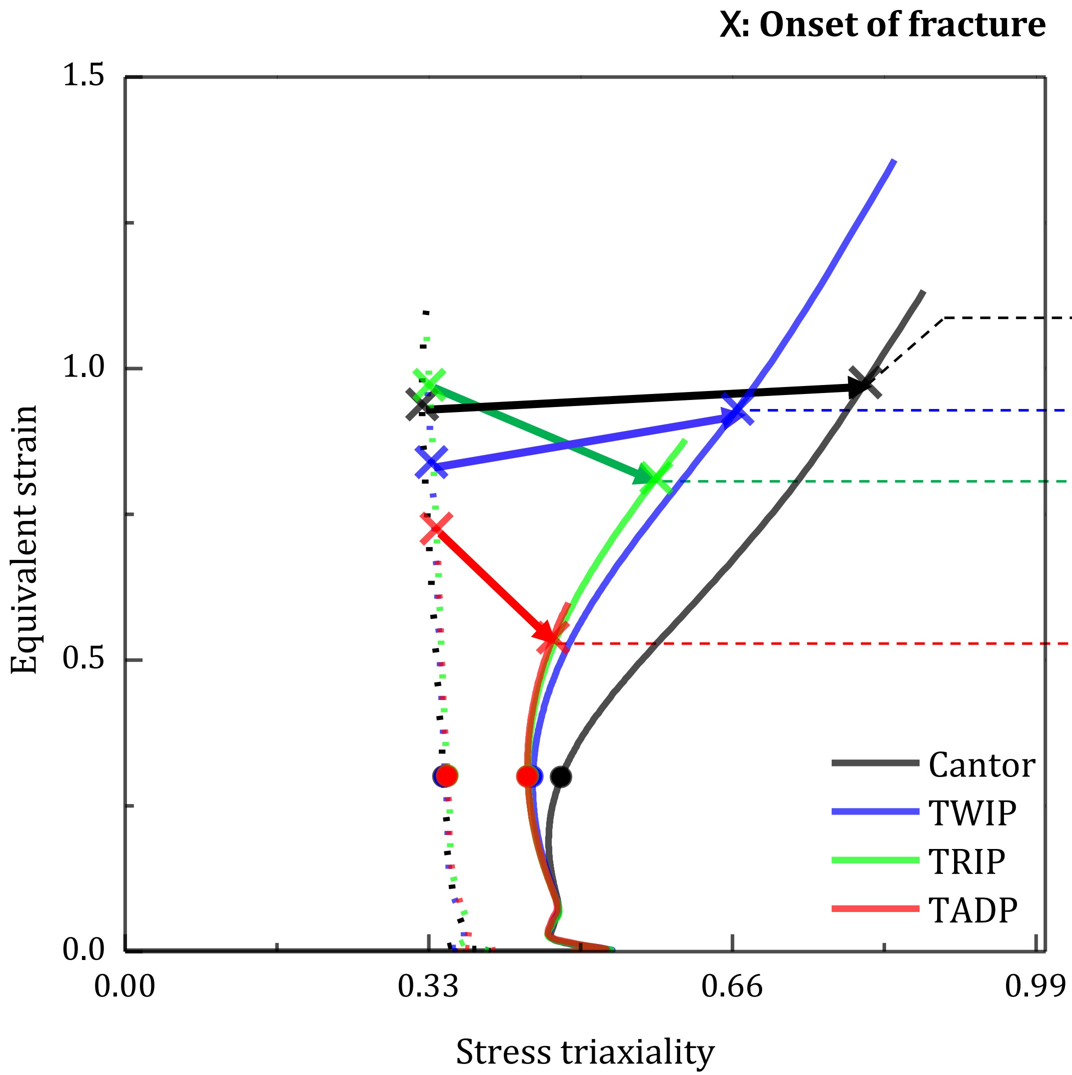

Cantor: Central hole < Notched test

TWIP: Central hole < Notched test

TRIP: Central hole > Notched test

TADP: Central hole > Notched test

For Phase transformation materials, equivalent strain is decreased

Fracture test: interrupt test at equivalent strain = 0.3

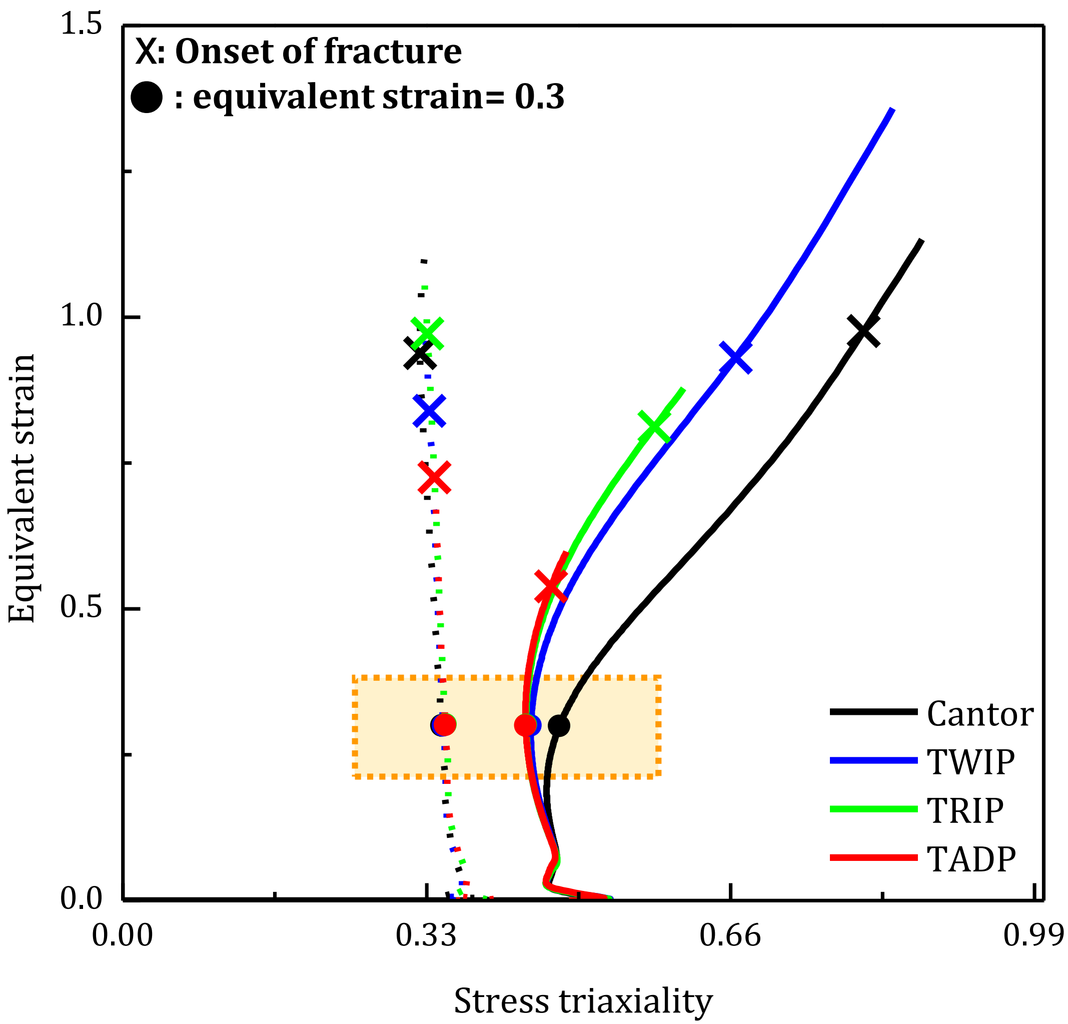

- **equivalent plastic strain**
  - Central hole

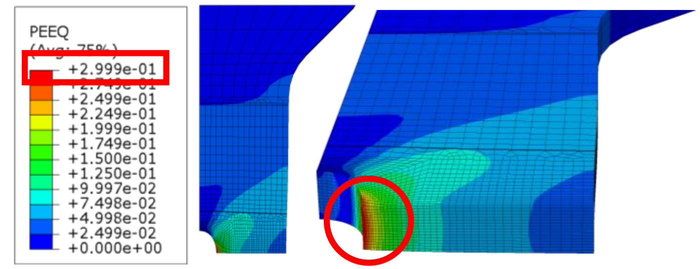

  - Notched test

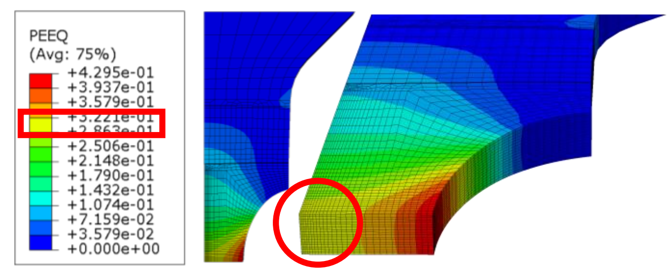

- **Displacement at equivalent strain = 0.3**

	Central hole	Notched test
Cantor	1.133mm	2.517mm
TWIP	1.326mm	3.508mm
TRIP	1.388mm	3.565mm
Dual Phase	1.268mm	3.113mm

Identify displacement corresponding to ε_{eq} = 0.3 in each stress state

Fracture test: interrupt test at equivalent strain = 0.3

	Central hole	Notched test
Cantor	1.133mm	2.517mm
TWIP	1.326mm	3.508mm
TRIP	1.388mm	3.565mm
Dual Phase	1.268mm	3.113mm

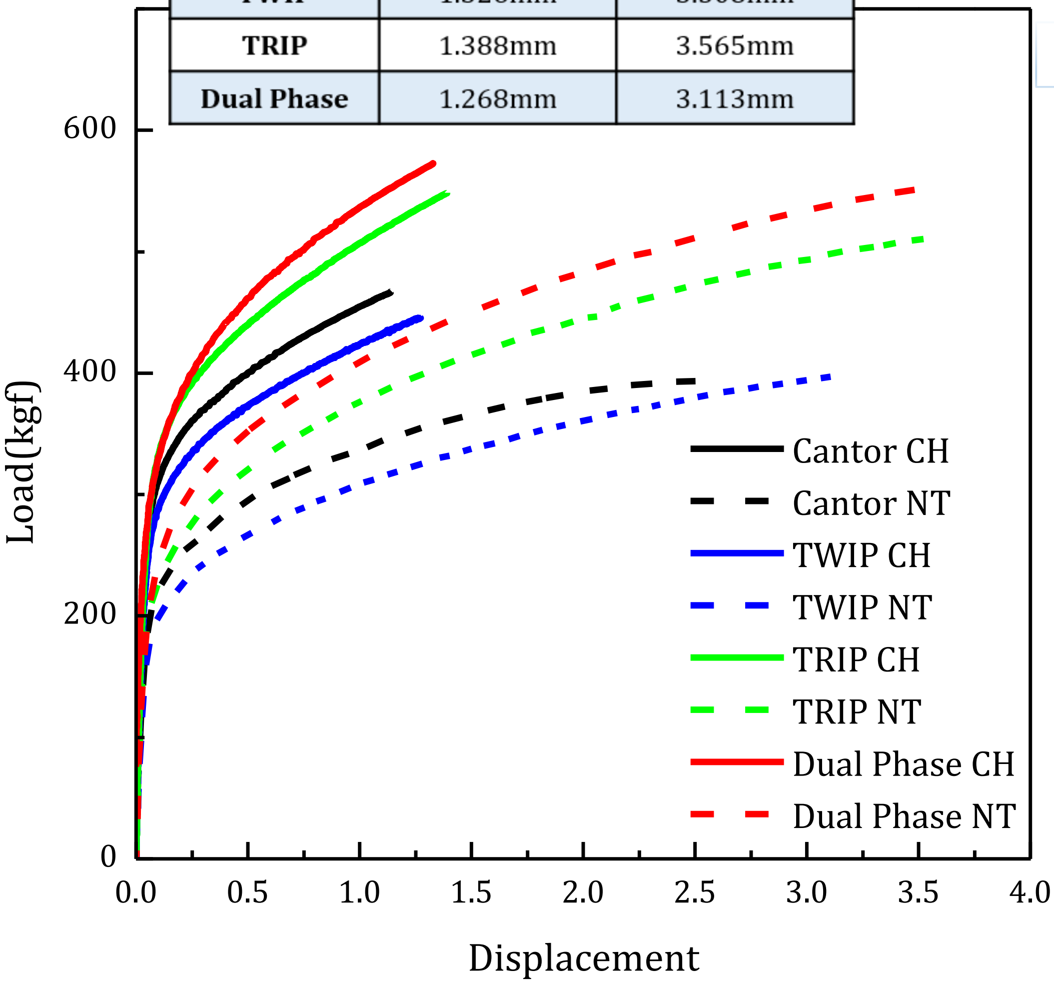

- **Central hole**

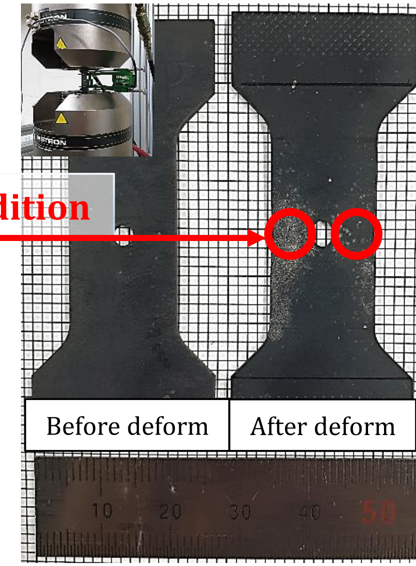

Uniaxial strain condition

- **Notched test**

Plane to biaxial strain condition

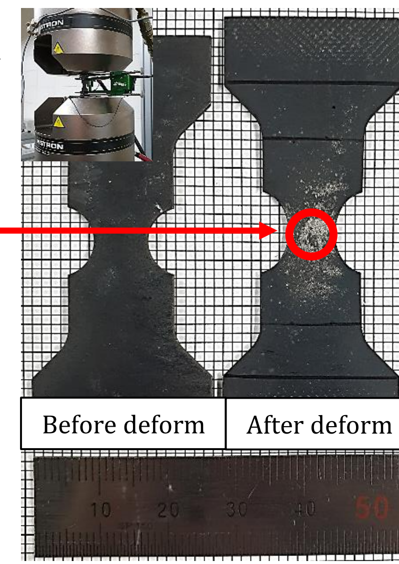

Fracture test was interrupted to compare the deformation behavior

Deformation behavior depending on stress state: TWIP

K. Renard et al. / Scripta Materialia 66 (2012) 966–971

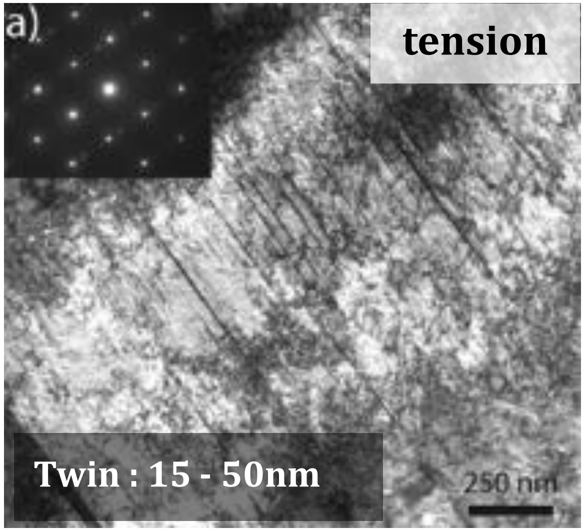

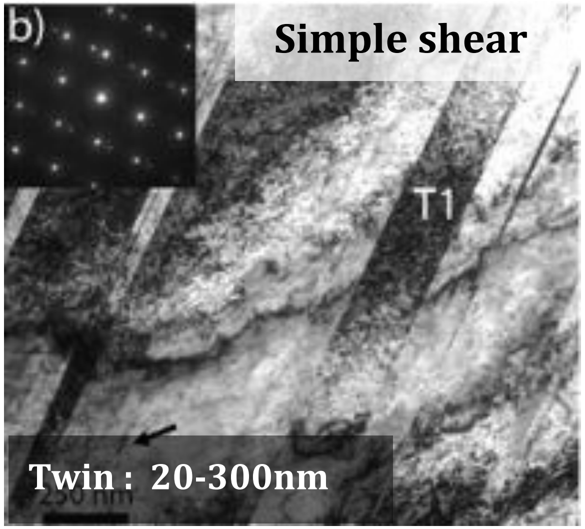

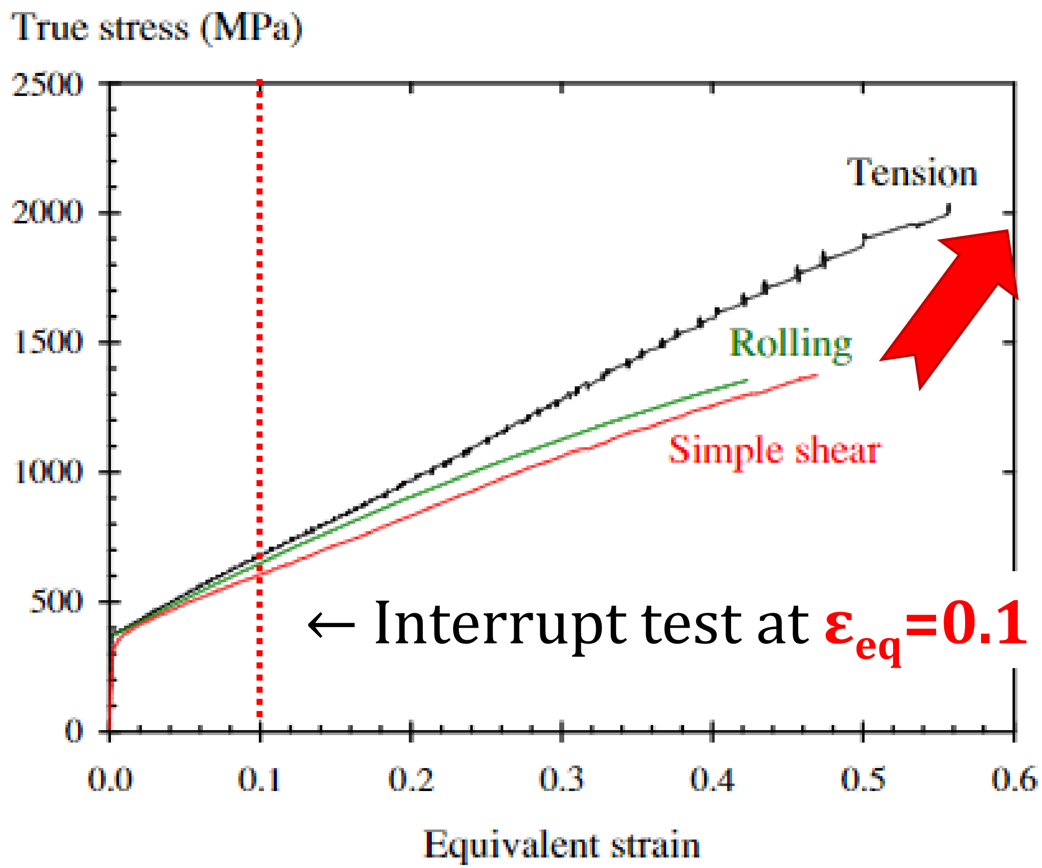

These two micrographs reveals a difference in the thickness of twin as a function of the stress state

Thickness of twins, influences their plastic behavior

Interrupted Fracture test: TWIP

Central hole : stress state(η=0.33)

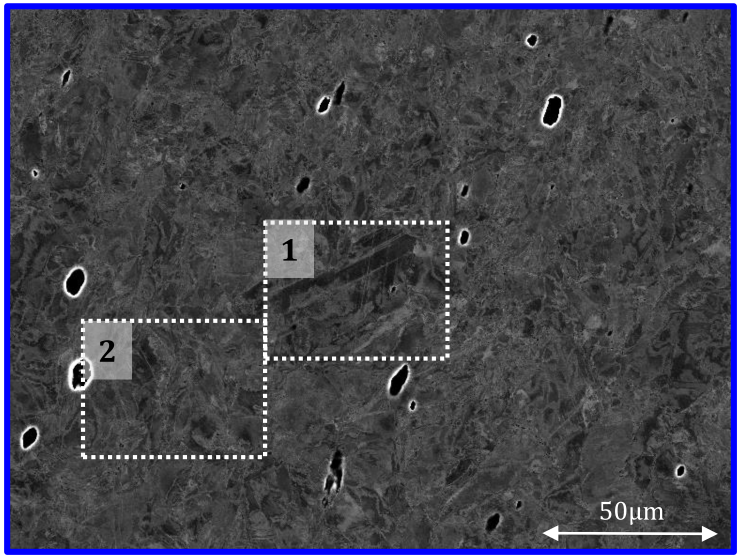

Notched test : stress state(η=0.33~0.66)

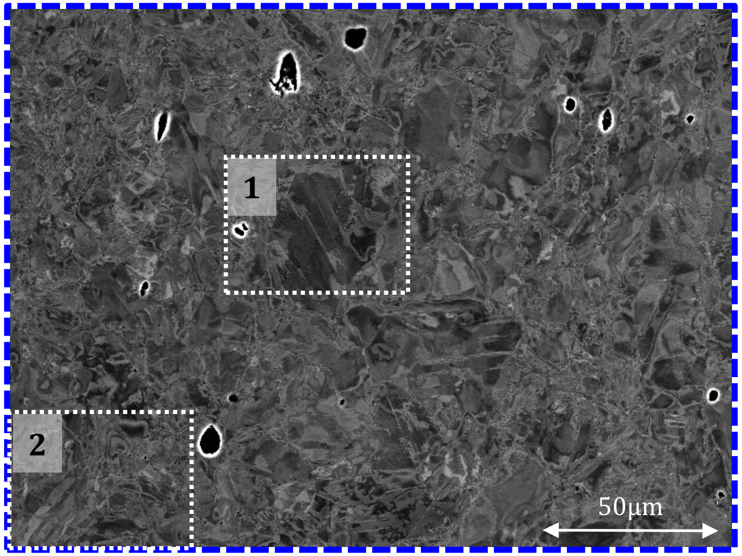

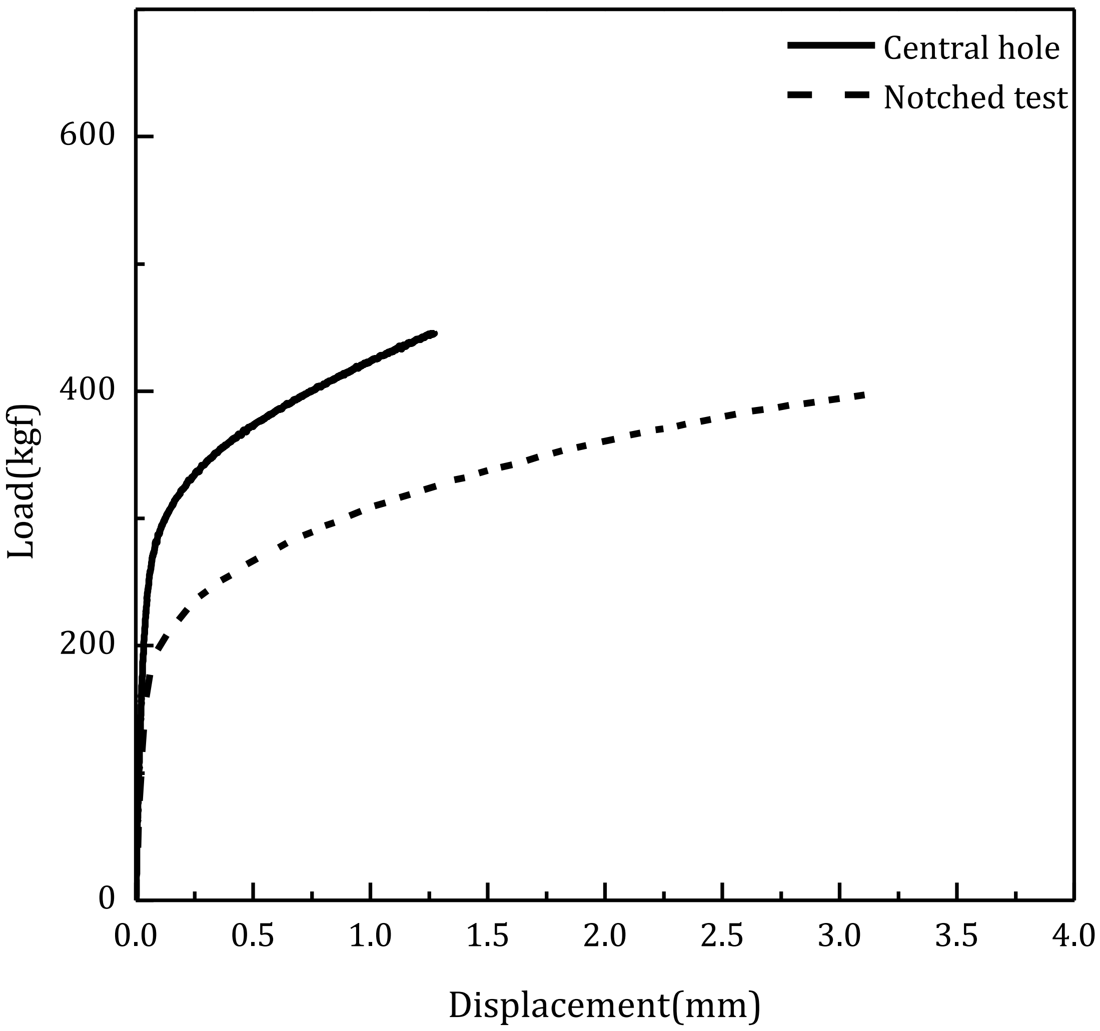

- Electron channeling contrast imaging(ECCI) of TWIP **Central hole test**

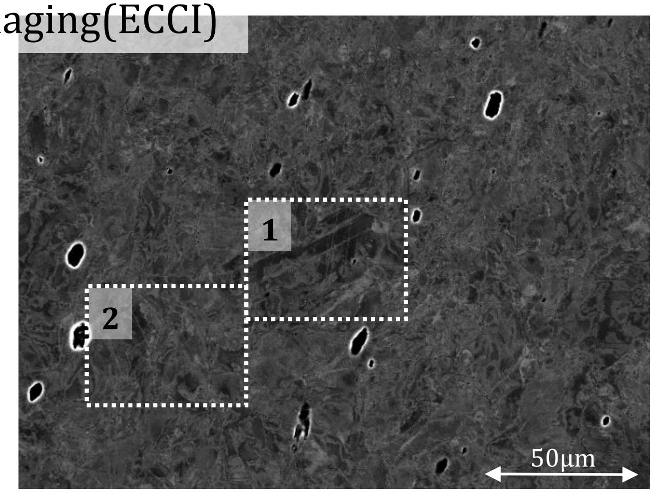

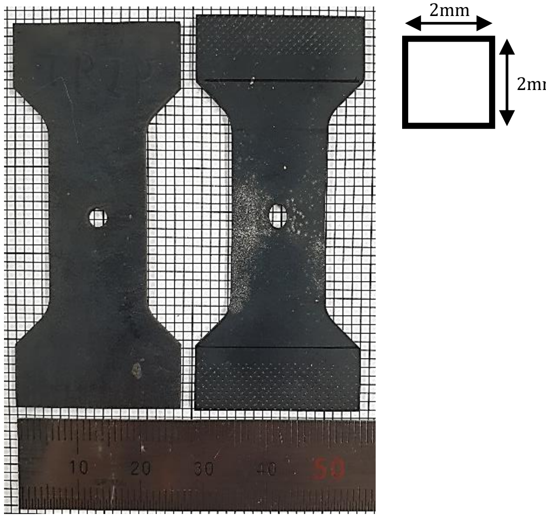

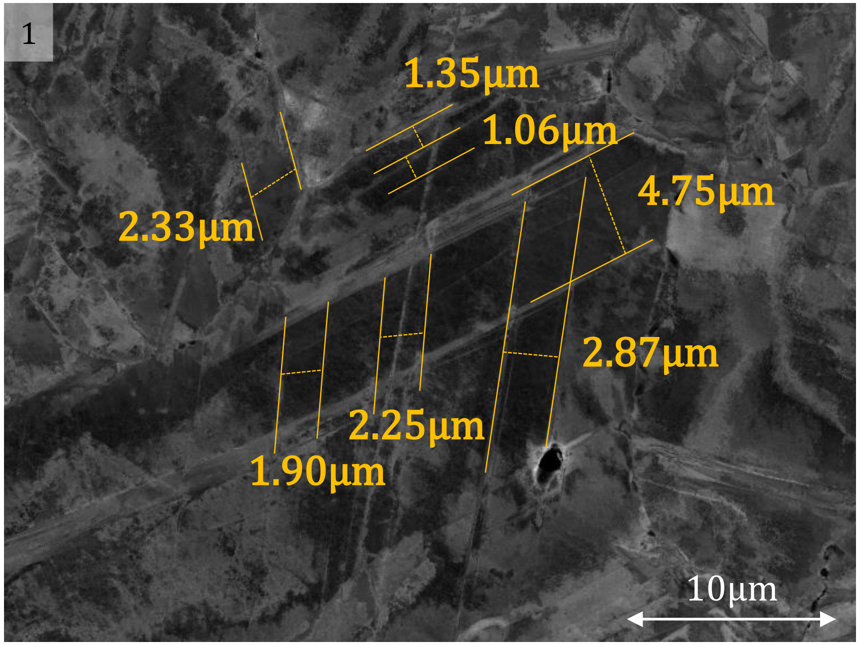

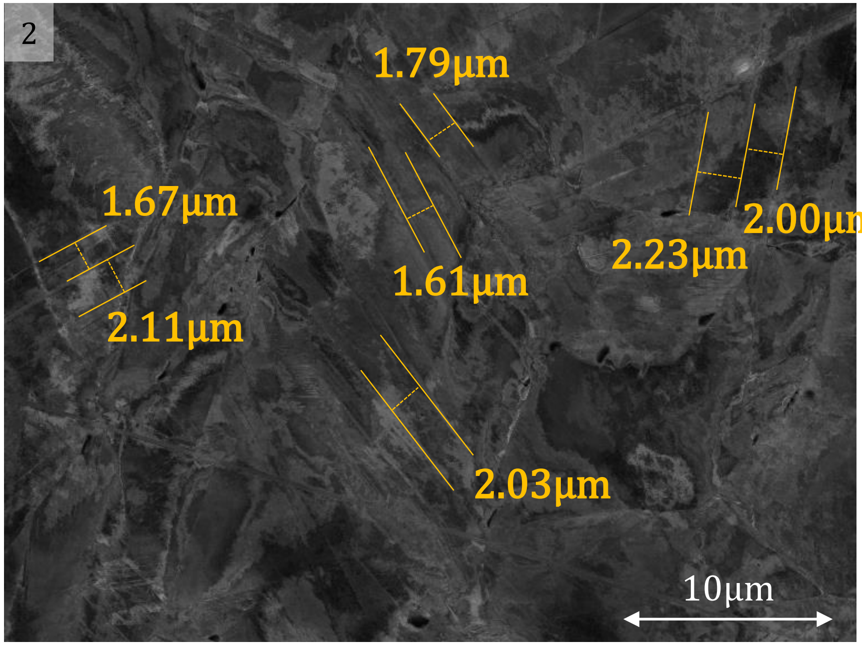

For central hole test(η=0.33), thickness of twins = 2.139μm ± 1μm

Interrupted Fracture test: Notched test(TWIP)

- Electron channeling contrast imaging(ECCI) of TWIP **Notched test**

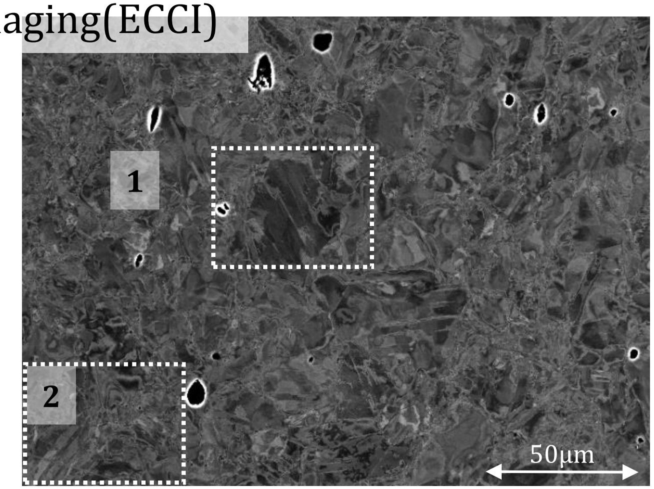

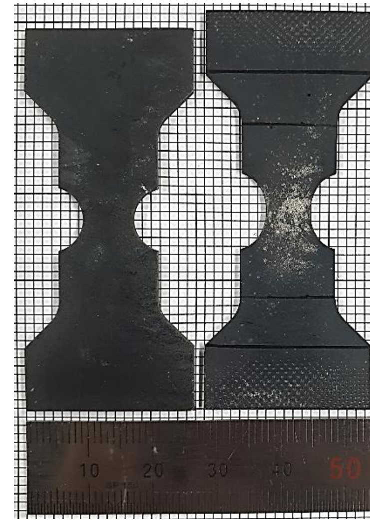

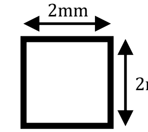

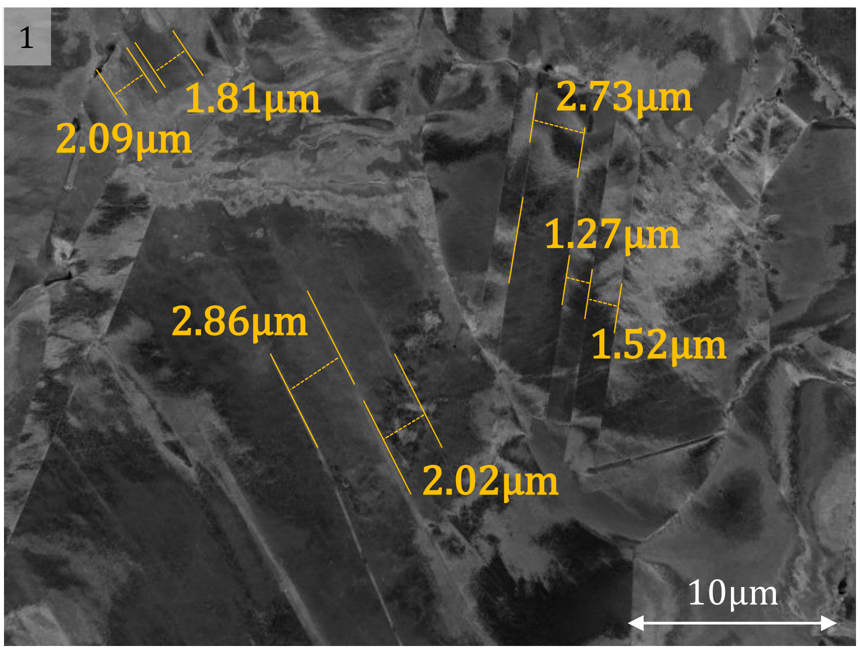

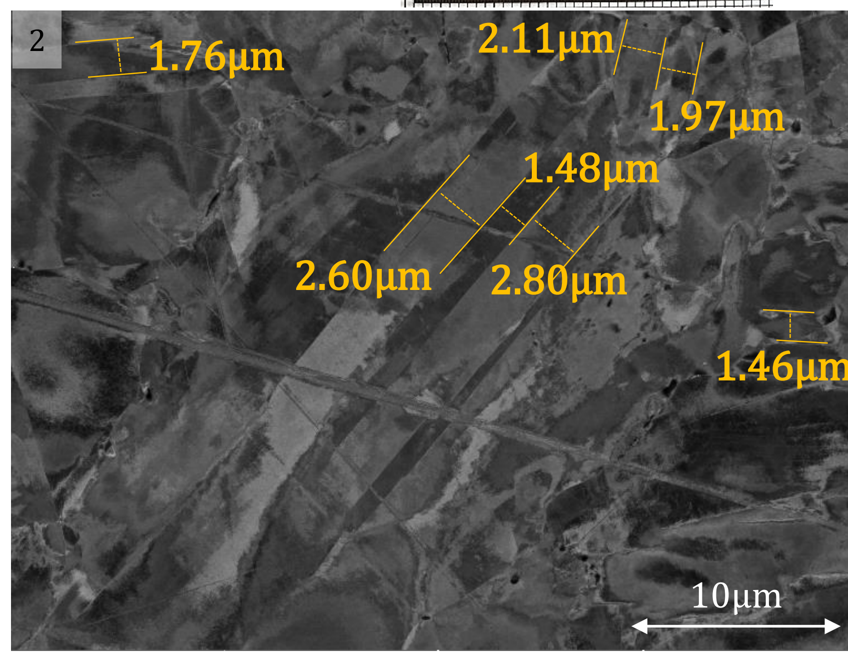

For Notched test(η=0.33~0.67), thickness of twins = 2.03μm ± 0.73μm

Central hole

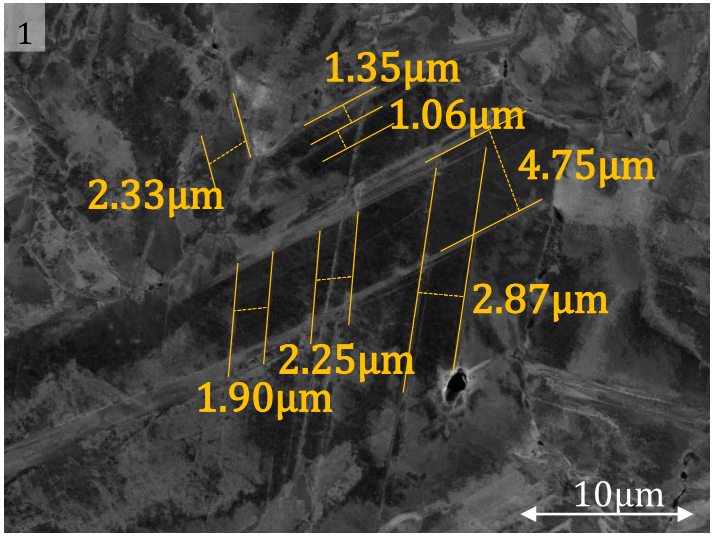

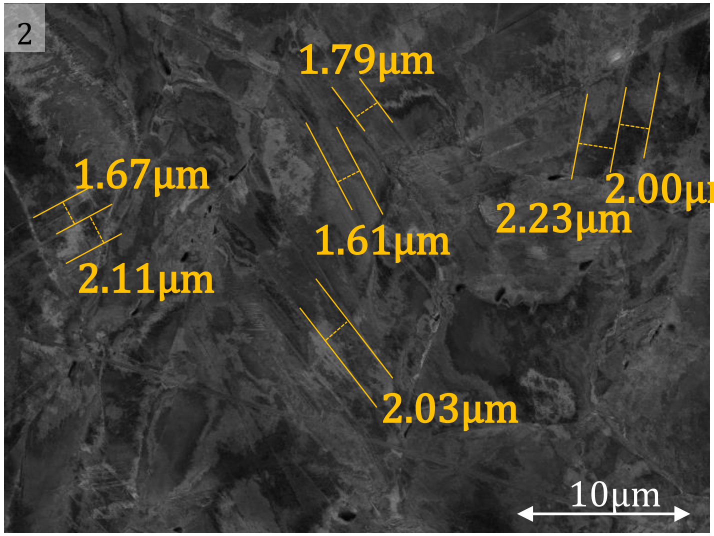

Notched test

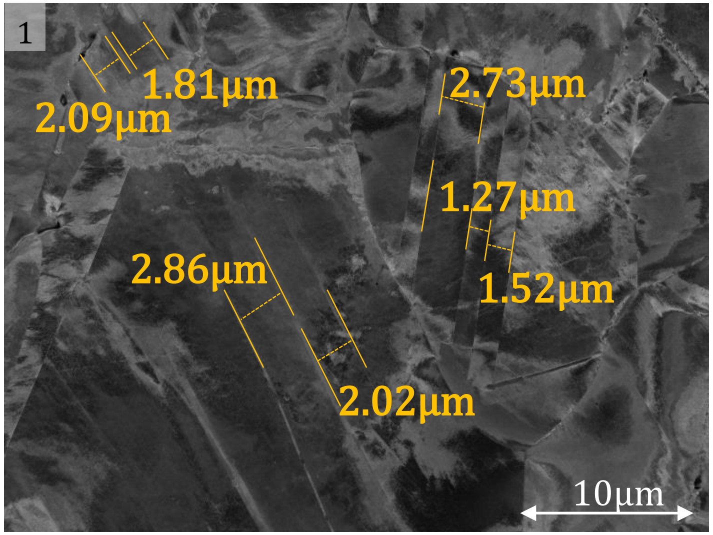

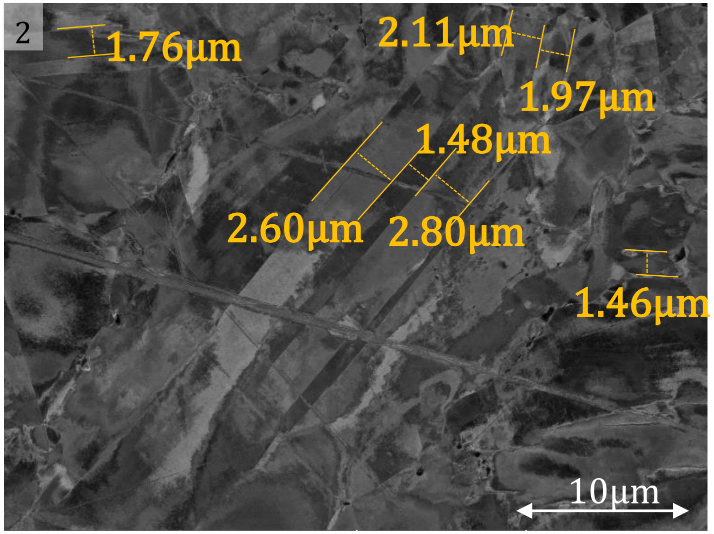

Twinning thickness of central hole and notched test is similar

Interrupted Fracture test: TRIP

- **Phase map of TRIP**

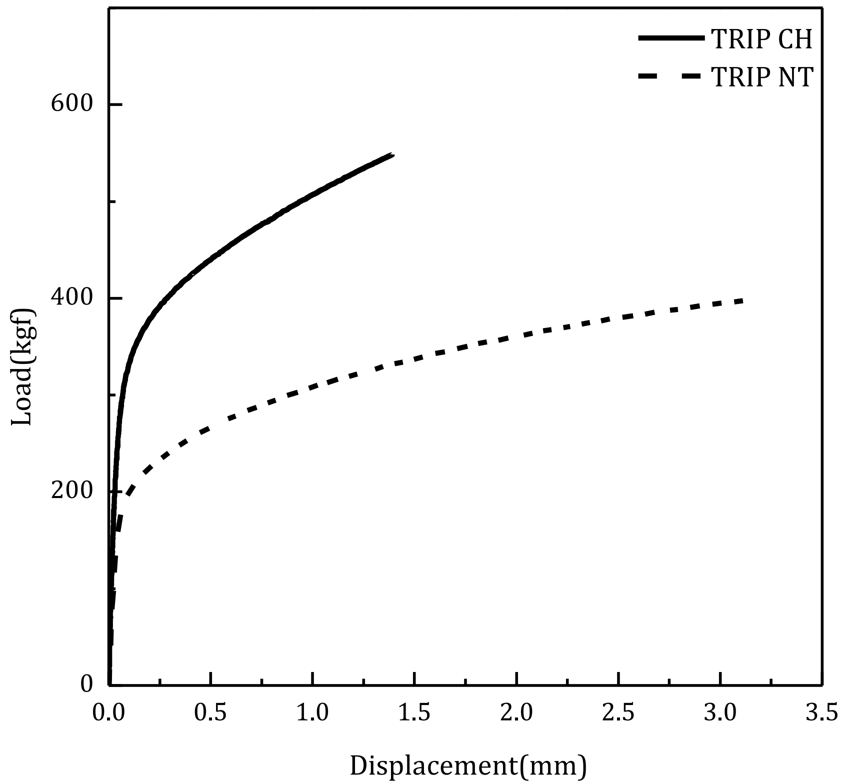

	Phase name	Central hole	Notched test
	Austenite(γ)	67%	80%
	Martensite(ε)	**33%**	**20%**

Central hole : stress state(η=0.33)

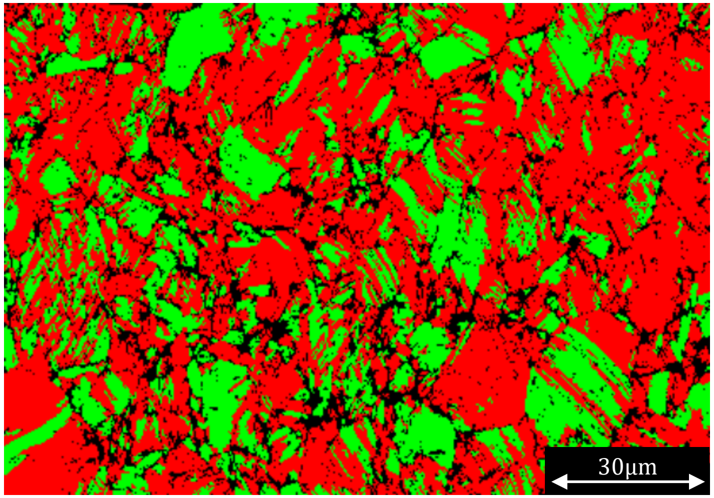

Notched test : stress state(η=0.33~0.66)

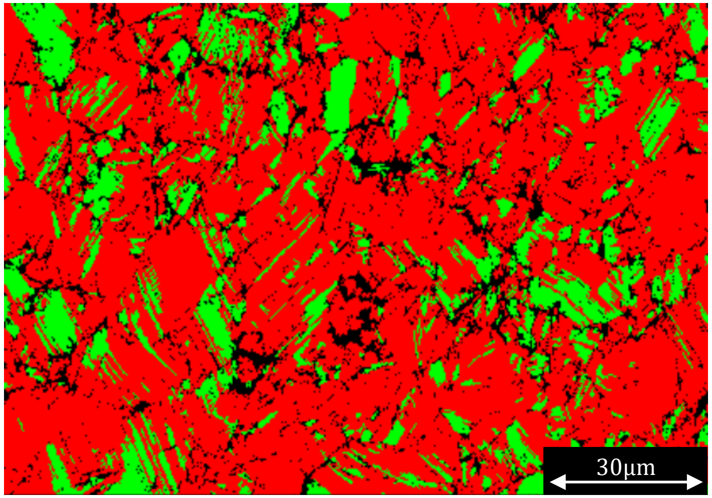

Phase transformation is occurred more easily in central hole

- **Phase map of TADP**

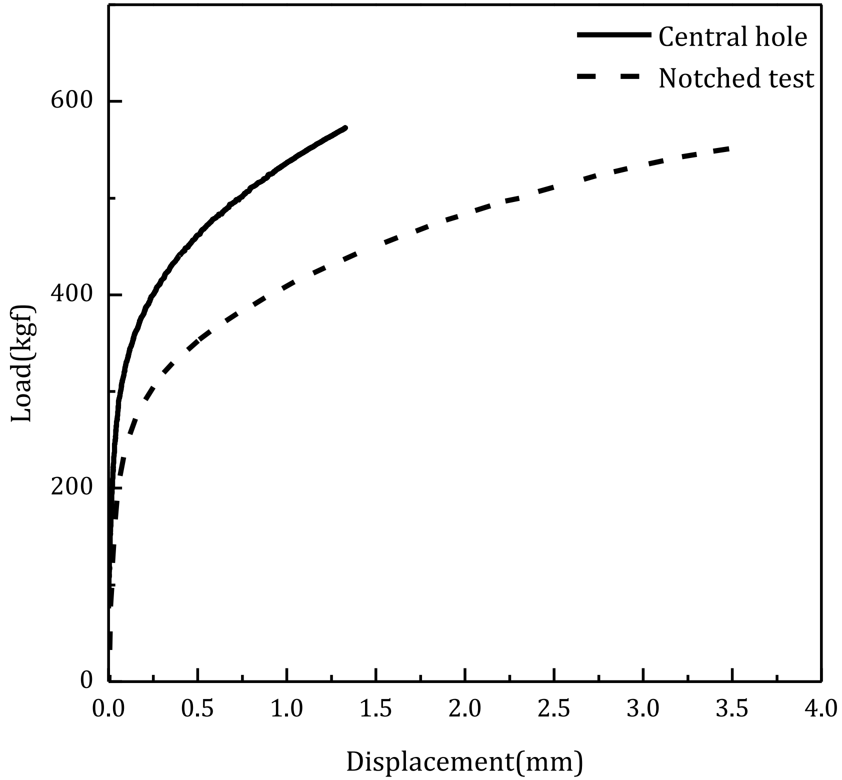

	Phase name	Central hole	Notched test
(red)	Austenite(γ)	39.7%	45.5%
(green)	Martensite(ε)	**60.3%**	**54.5%**

Central hole : stress state(η=0.33)

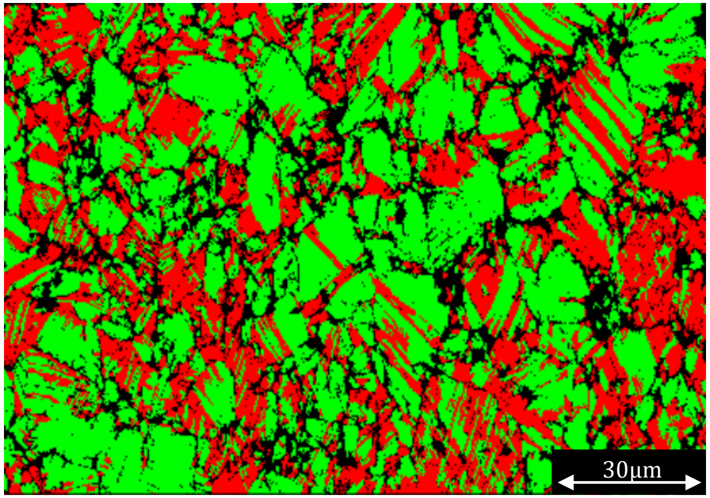

Notched test : stress state(η=0.33~0.66)

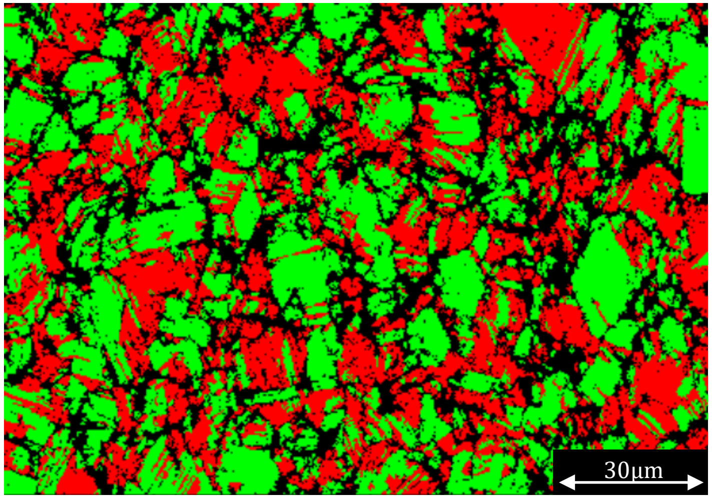

Phase transformation is occurred more easily in central hole

Interrupted Fracture test: TRIP & TADP

TRIP

Central hole

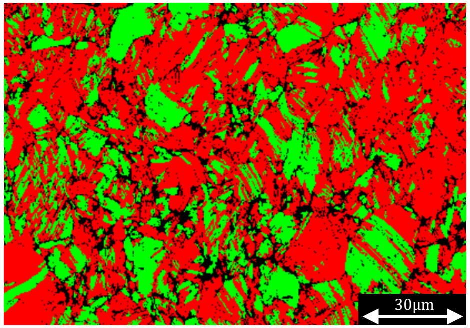

Notched test

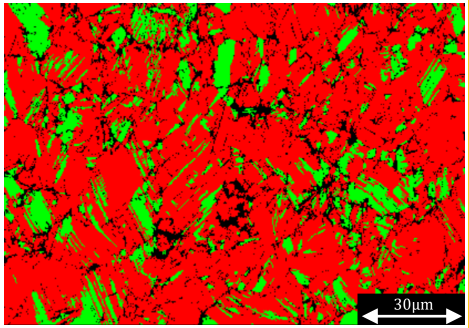

	Phase name	Central hole	Notched test
	Austenite(γ)	67%	80%
	Martensite(ε)	**33%**	**20%**

TADP

Central hole

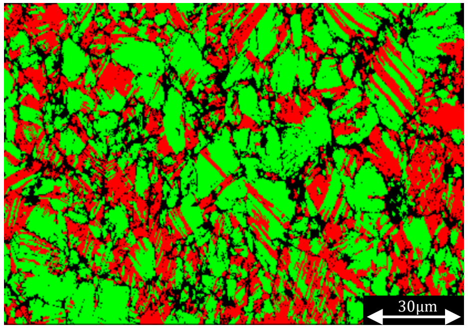

Notched test

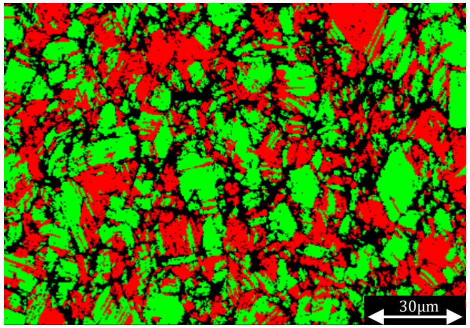

	Phase name	Central hole	Notched test
	Austenite(γ)	39.7%	45.5%
	Martensite(ε)	**60.3%**	**54.5%**

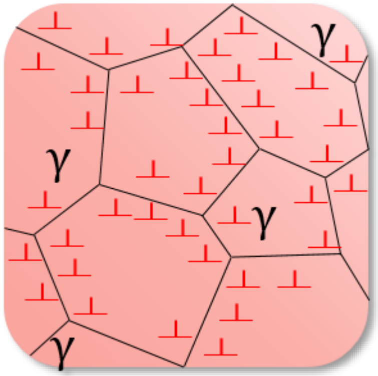

Dislocation gliding

\+

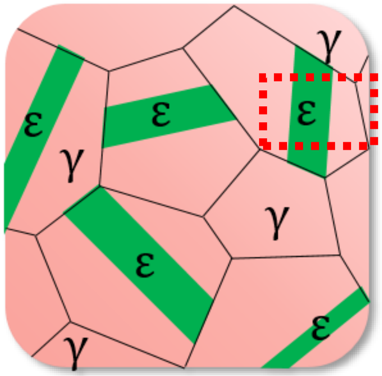

Phase transformation

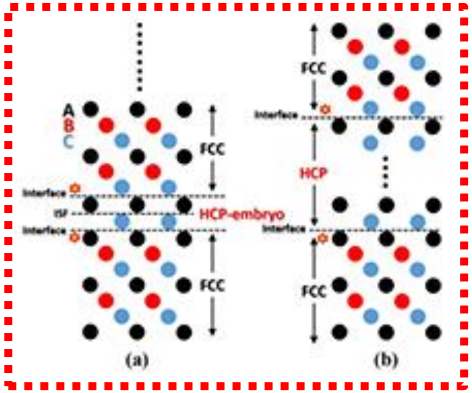

Additional plastic flow is obtained by M transformation in uniaxial stress state

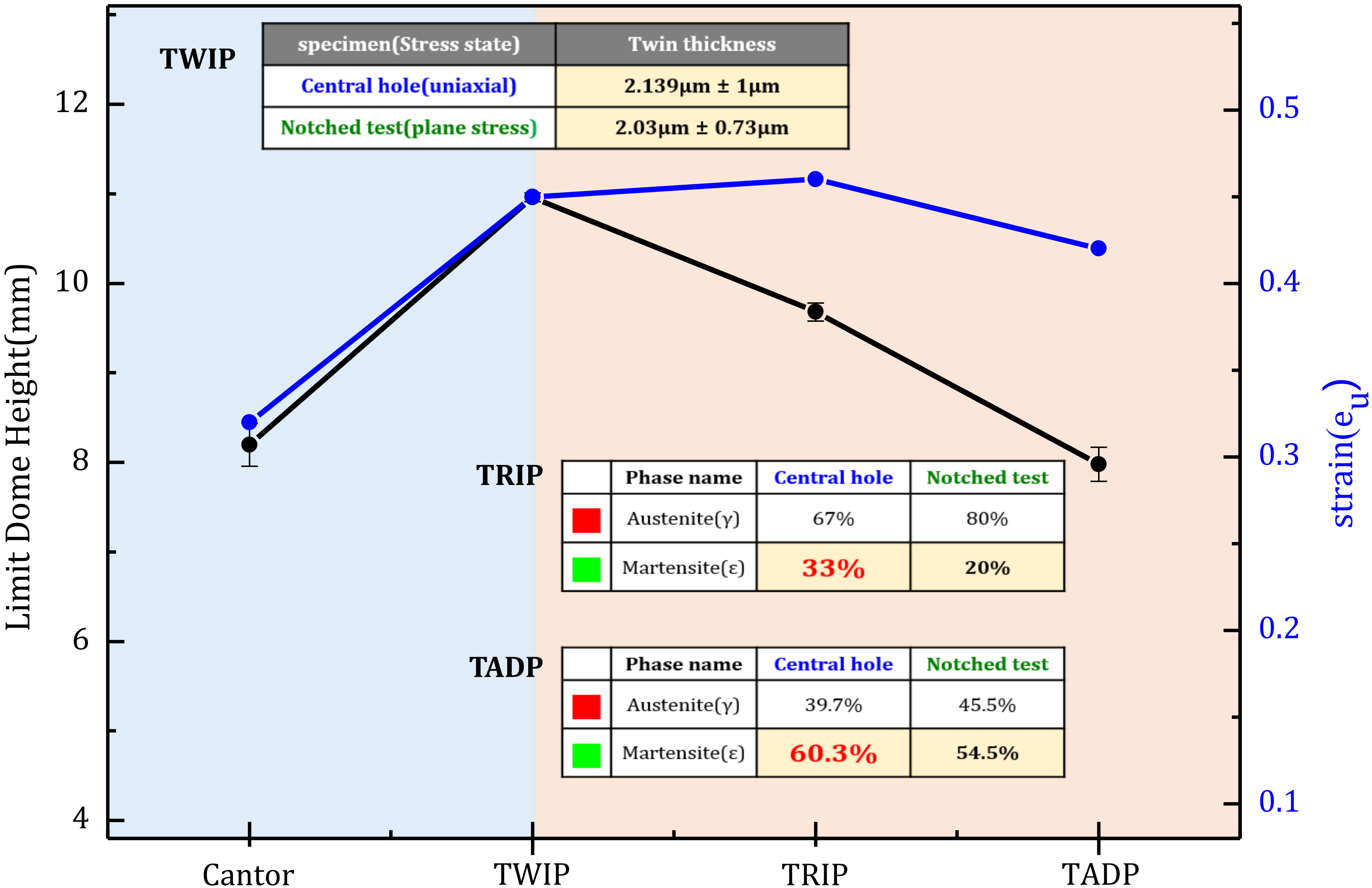

TWIP

specimen(Stress state)	Twin thickness
Central hole(uniaxial)	2.139μm ± 1μm
Notched test(plane stress)	2.03μm ± 0.73μm

TRIP

	Phase name	Central hole	Notched test
	Austenite(γ)	67%	80%
	Martensite(ε)	33%	20%

TADP

	Phase name	Central hole	Notched test
	Austenite(γ)	39.7%	45.5%
	Martensite(ε)	60.3%	54.5%

Composition of designed CCAs

#	Note	Composition	Deformation mechanism
-	Cantor	$Cr_{20}Mn_{20}Fe_{20}Co_{20}Ni_{20}$	Dislocation gliding
1	**CCA19**	$Cr_{20}Mn_{19}Fe_{21}Co_{21}Ni_{19}$	
2	**CCA18**	$Cr_{20}Mn_{18}Fe_{22}Co_{22}Ni_{18}$	
3	**CCA17**	$Cr_{20}Mn_{17}Fe_{23}Co_{23}Ni_{17}$	
4	**CCA16**	$Cr_{20}Mn_{16}Fe_{24}Co_{24}Ni_{16}$	
5	**CCA15**	$Cr_{20}Mn_{15}Fe_{25}Co_{25}Ni_{15}$	
-	TWIP	$Cr_{20}Mn_{14}Fe_{24}Co_{24}Ni_{16}$	Twinning
6	**CCA13**	$Cr_{20}Mn_{13}Fe_{27}Co_{27}Ni_{13}$	
7	**CCA12**	$Cr_{20}Mn_{12}Fe_{28}Co_{28}Ni_{12}$	
8	**CCA11**	$Cr_{20}Mn_{11}Fe_{29}Co_{29}Ni_{11}$	
-	TRIP	$Cr_{20}Mn_{10}Fe_{30}Co_{30}Ni_{10}$	Phase transformation
-	TADP	$Cr_{20}Mn_{8}Fe_{32}Co_{32}Ni_{8}$	Phase transformation

New series of CCAs is designed by changing the composition

True stress strain curve of designed CCAs

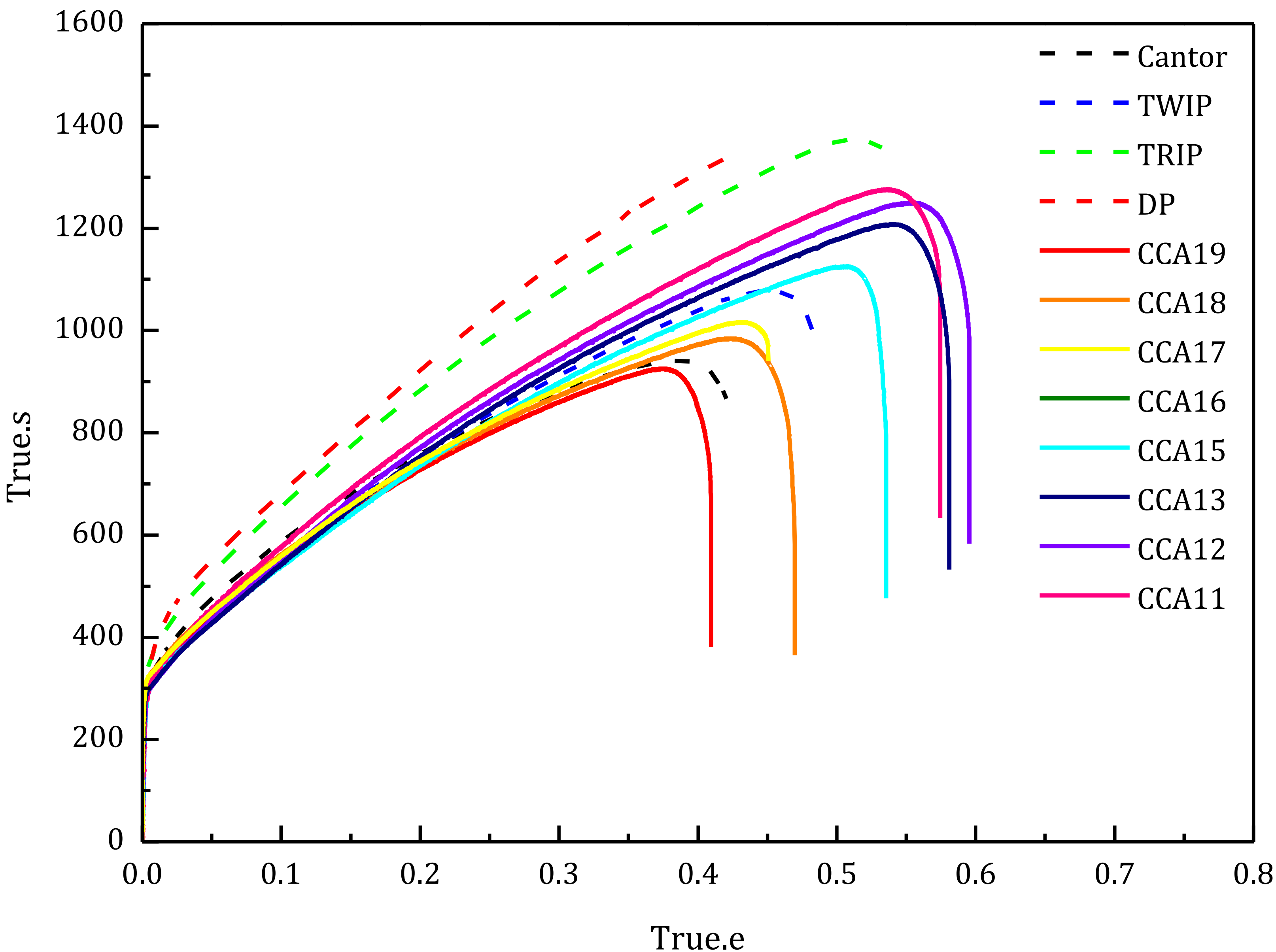

Uniform elongation summary of designed CCAs

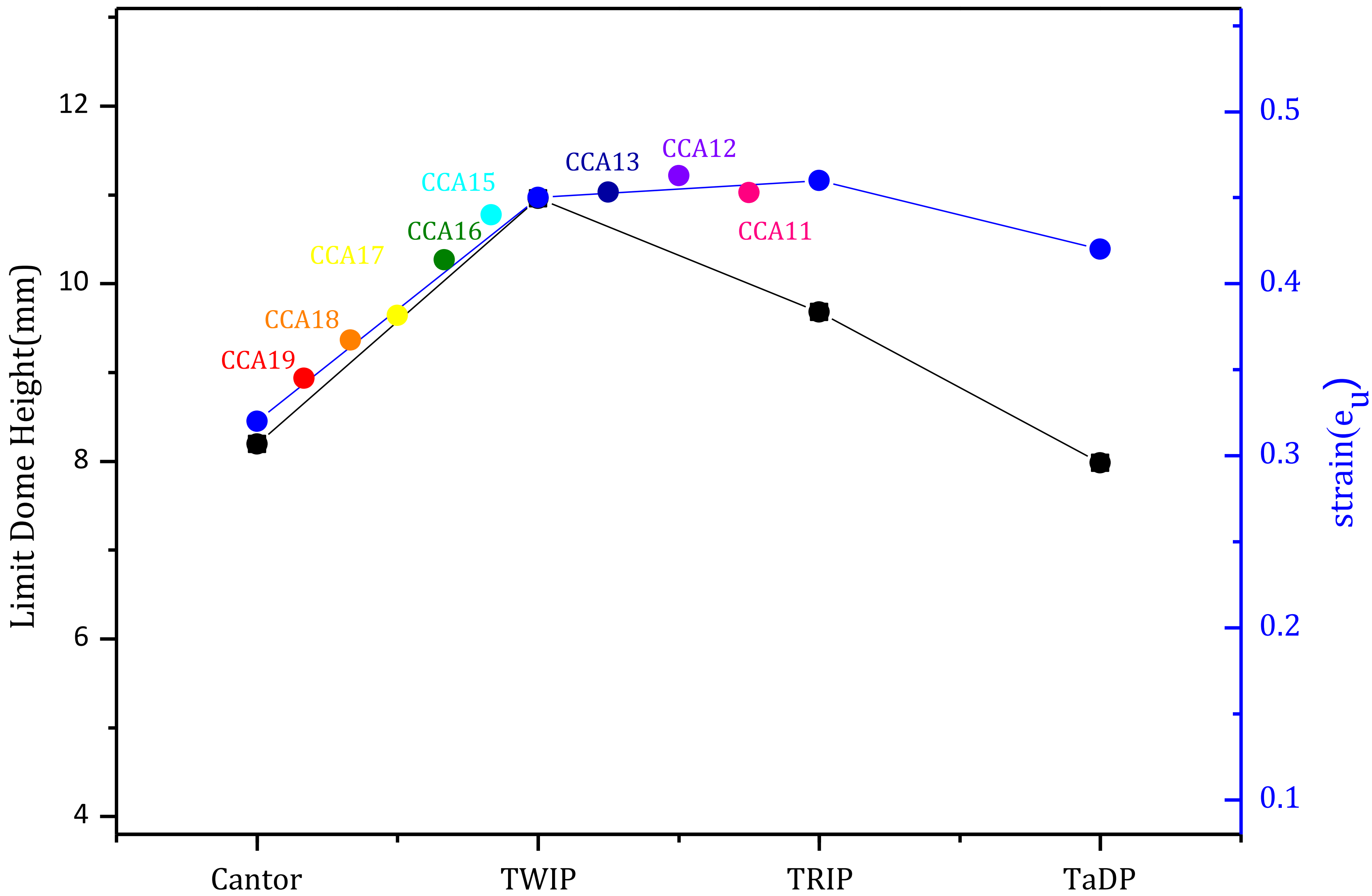

Deformation mechanism of designed CCA

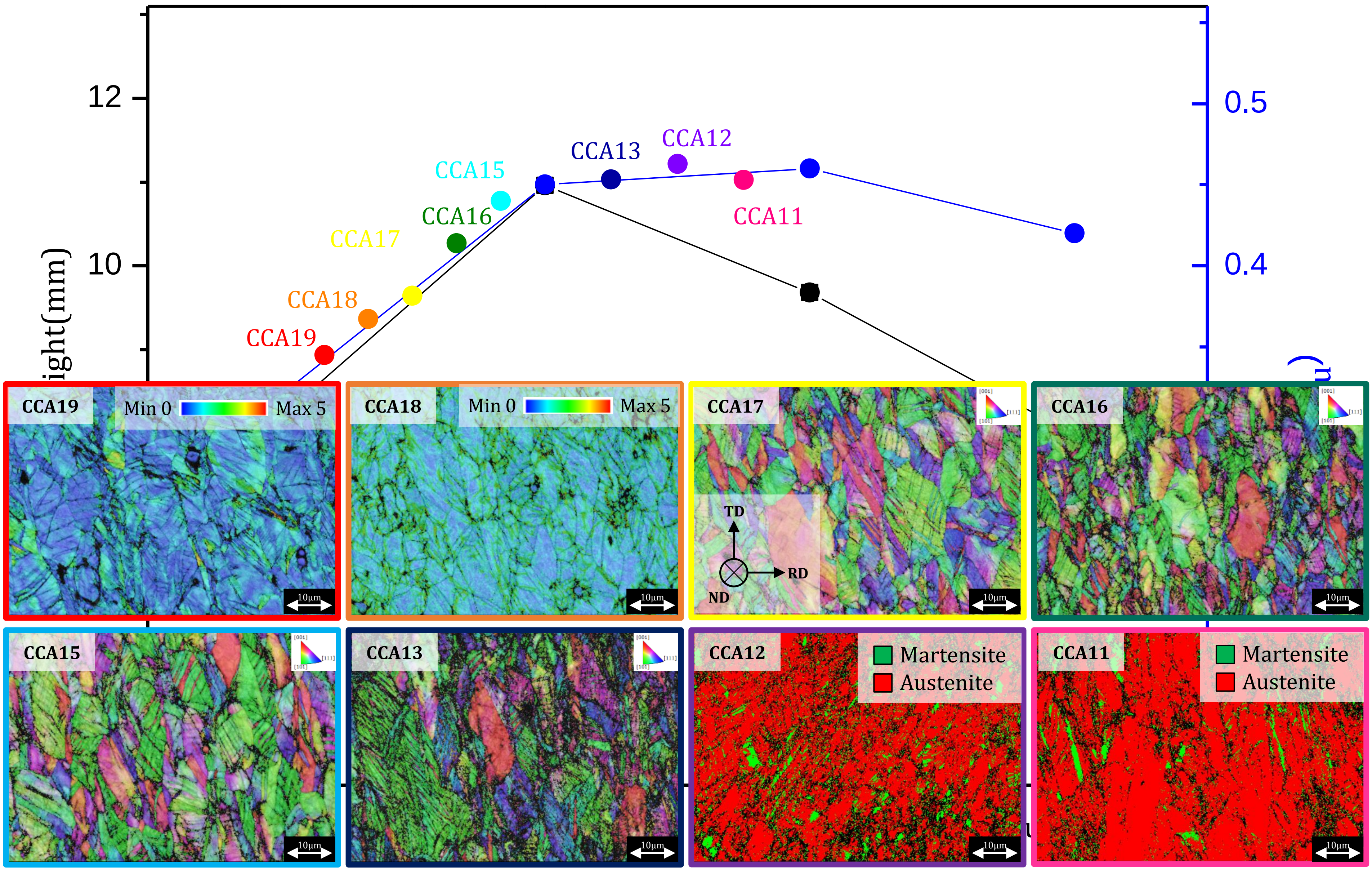

Summary – *Designed CCAs* with enhanced formability

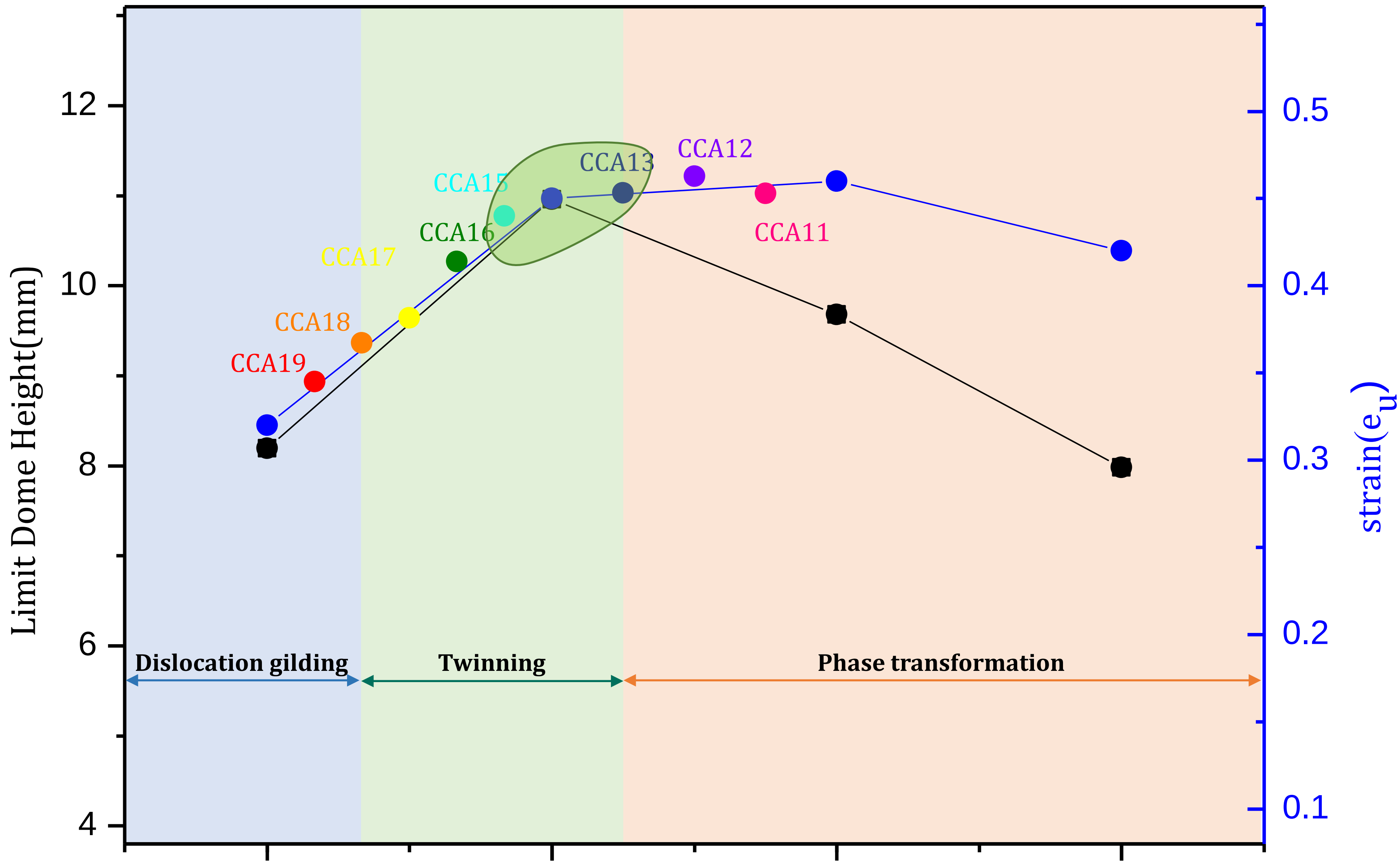

CCA15, TWIP, and CC13 is expected to have good formability

1. Formability test

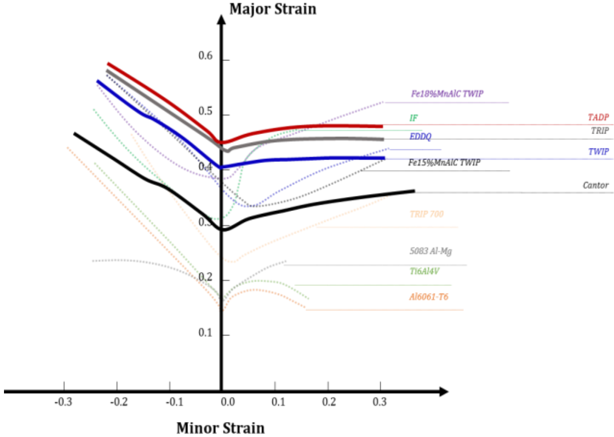

FLD: Cantor < TWIP < TRIP < TADP
Strain localization

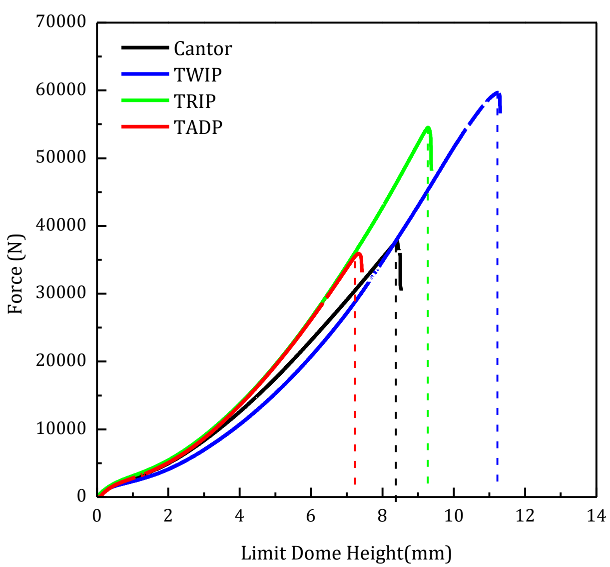

LDH: TWIP < TRIP < Cantor < TADP
Strain localization + Post necking region

2. Fracture test

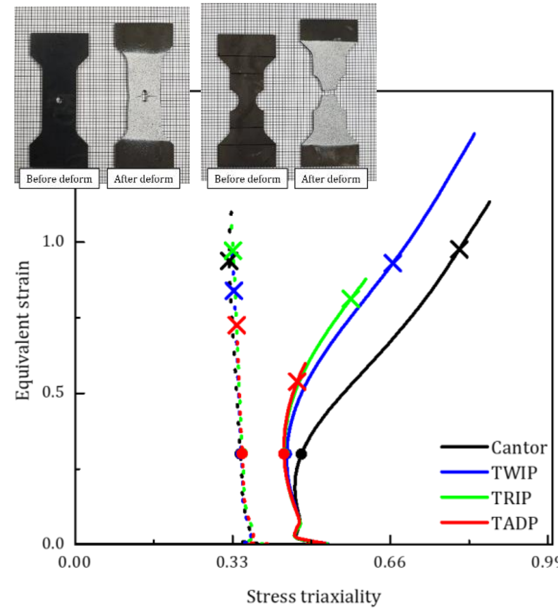

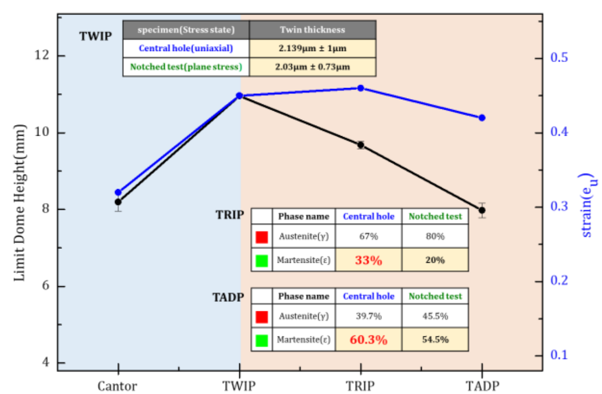

TWIP

specimen(Stress state)	Twin thickness
Central hole(uniaxial)	2.139μm ± 1μm
Notched test(plane stress)	2.03μm ± 0.73μm

TRIP

Phase name	Central hole	Notched test
Austenite(γ)	67%	80%
Martensite(ε)	33%	20%

TADP

Phase name	Central hole	Notched test
Austenite(γ)	39.7%	45.5%
Martensite(ε)	60.3%	54.5%

TWIP: Twinning thickness of central hole and notched test is similar

TRIP, TADP: Phase transformation is occurred more easily in central hole

3. Alloy design

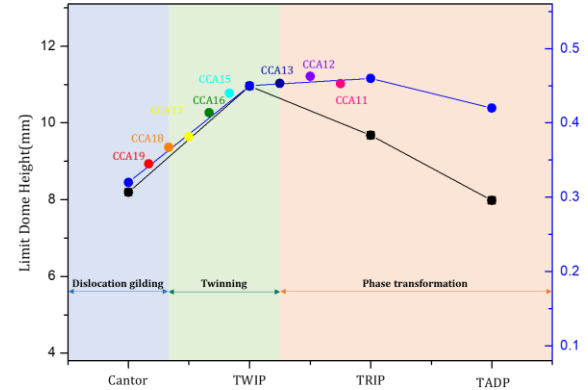

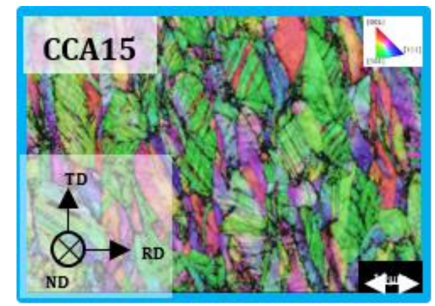

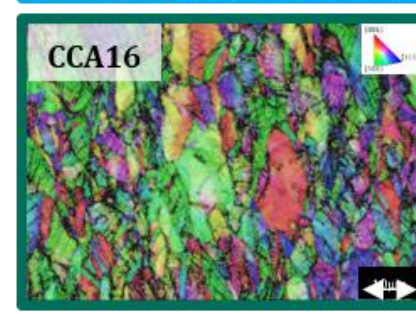

- **Twinning material follows the uniaxial strain tendency during forming**
- **CCA15, TWIP, and CC13 is expected to have good formability**

Thank you for your kind attention